האוניברסיטה העברית בירושלים
THE HEBREW UNIVERSITY OF JERUSALEM

Noemie Globus

On UHECRs Origin

work in collaboration with

T. Piran (HUJI, Israel),
D. Eichler (BGU, Israel),
D. Allard (APC, Paris),
E. Parizot (APC, Paris),
C. Lachaud (APC, Paris),
R. Mochkovitch (IAP, Paris)

UHECR Observatories

the cosmic-rays 4 CR/cm2/s => 1 kg/year
UHECRs : 1 part/km2/century

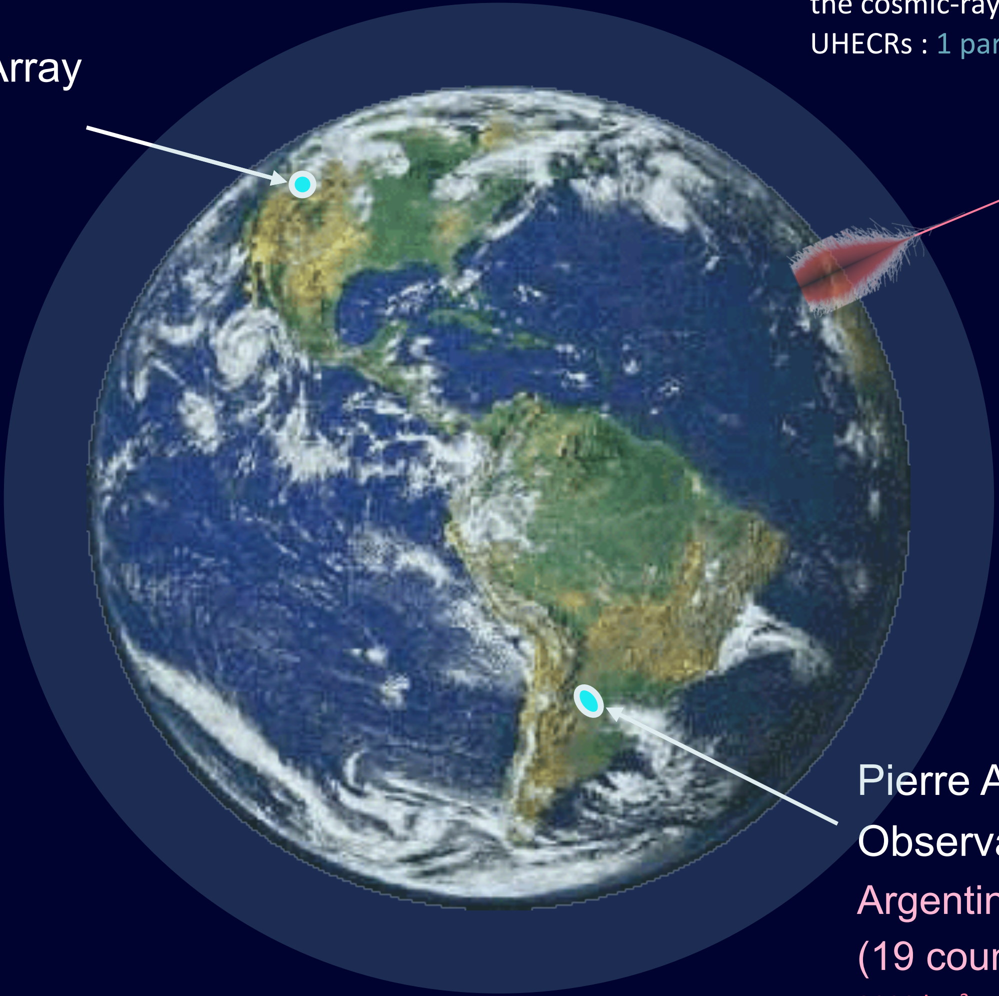

Telescope Array
Utah, USA
(5 countries)
700 km^2 array
3 fluorescence telescopes

Pierre Auger Observatory
Argentina
(19 countries)
3000 km^2 array
4 fluorescence telescopes

Cosmic Rays primary observables

Energy spectrum

↓

Differential flux

Mass spectrum

↓

composition

Angular spectrum

↓

Arrival direction

Situation at ultra high energy : recent results of PAO and TA

Auger Anisotropy Data Set (ApJ 804 15, 2015**)**

SD data from period **1.01.2004 — 31.03.2014** (10 years)

Zenith angle up to 80°

Exposure **66,452 km² yr sr**

- 231 above 52 EeV

Angular resolution: better than 0.9°

Energy resolution: 14%

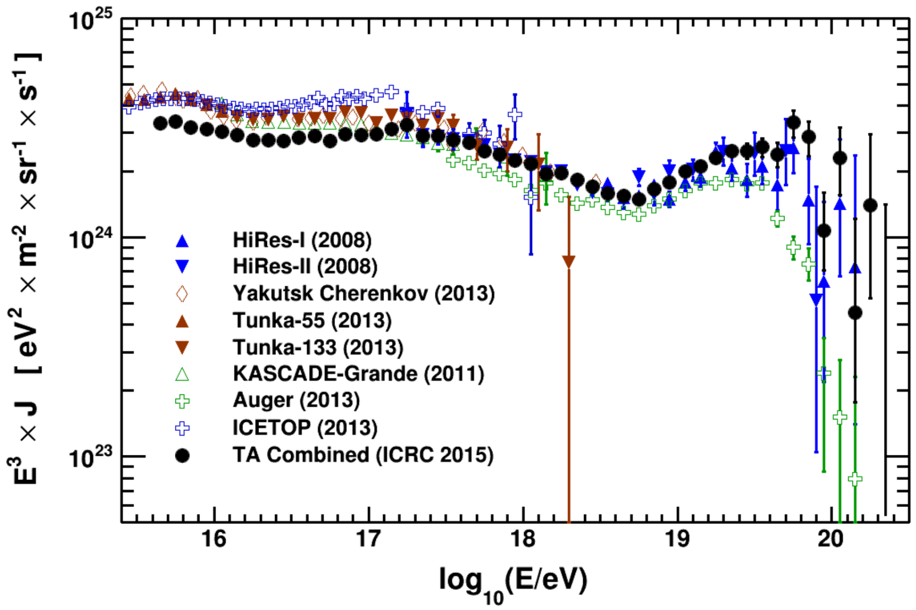

Situation at ultra high energy : recent results of PAO and TA

TA Anisotropy Data Set (John Matthews' talk, ICRC 2015)

SD data from period **12.05.2008 — 11.05.2015** (7 years)

Zenith angle up to 55°, loose border cut

Exposure **8,600 km² yr sr**

- 83 above 57 EeV

Angular resolution: better than 1.5°

Energy resolution: 20%

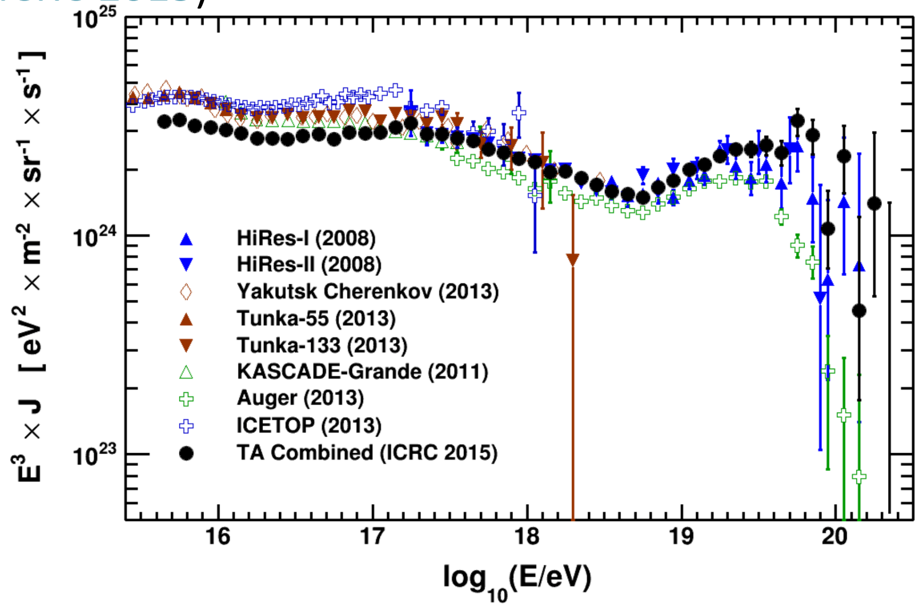

Situation at ultra high energy : recent results of PAO and TA

Both experiments observe two features in the spectrum:

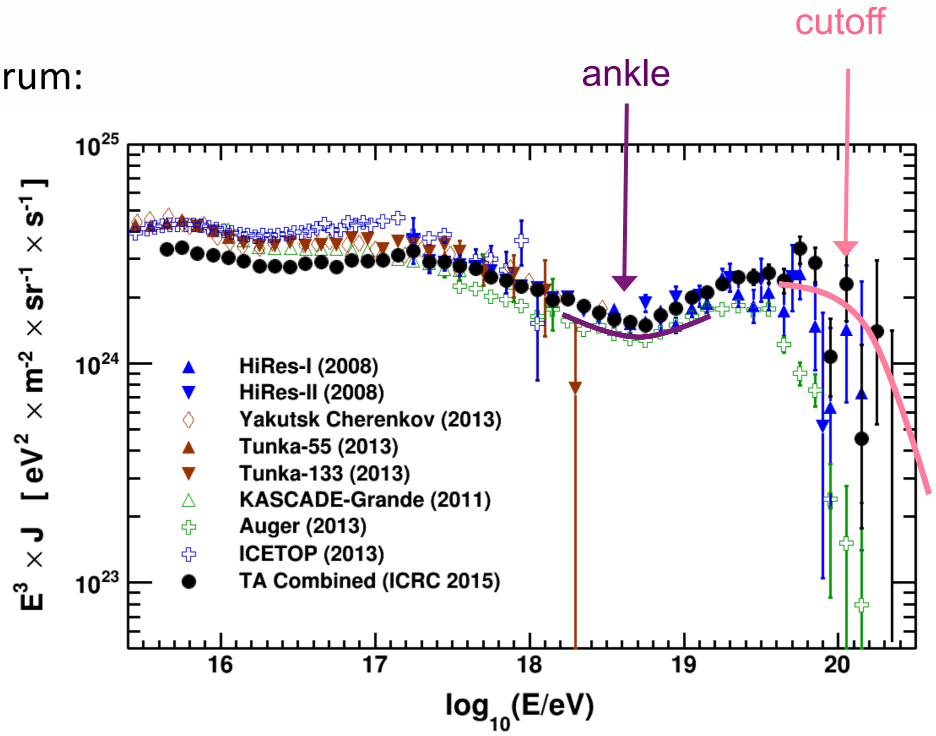

- an ankle at ~3–5 10^{18} eV
- a "cutoff" at ~3 10^{20} eV

How do we interpret them?

- UHE cosmic-rays are thought to be extragalactic

- they must travel huge distance from their source to the Earth

- they might loose energy (expansion of the Universe, interactions)

- baryonic matter density extremely low

=> p-p or p-N interactions are negligible

- what about photo-interactions ?

There is a upper limit on the energy of cosmic rays coming from distant sources (Greisen–Zatsepin–Kuzmin limit)

The GZK attenuation length: pure proton case

Proton attenuation length

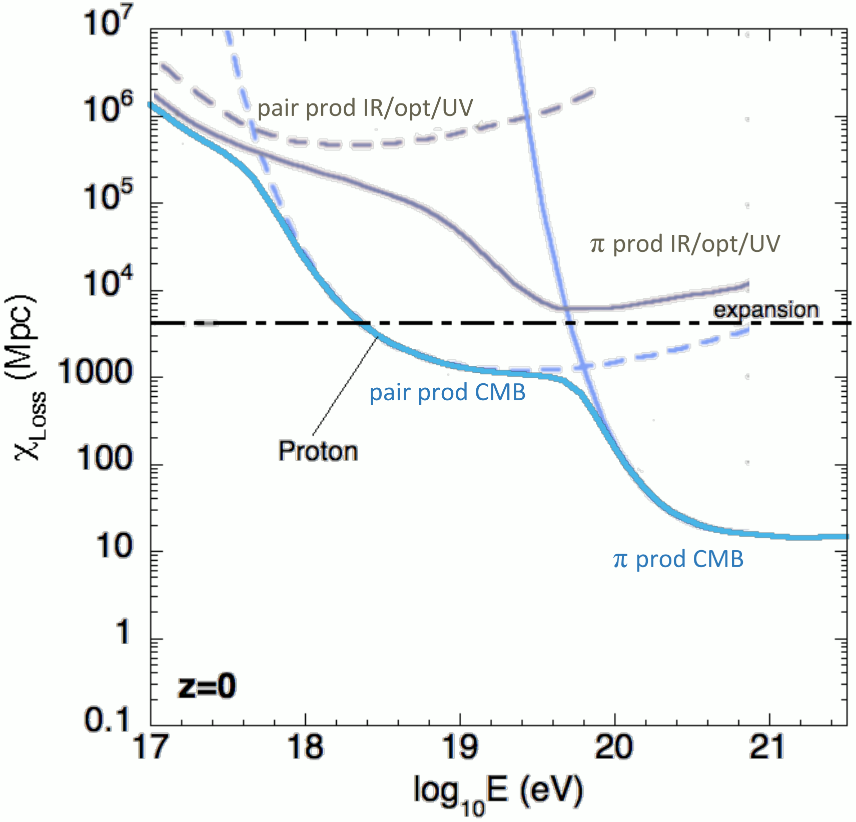

Calculation of the propagated spectrum (Allard 2005)

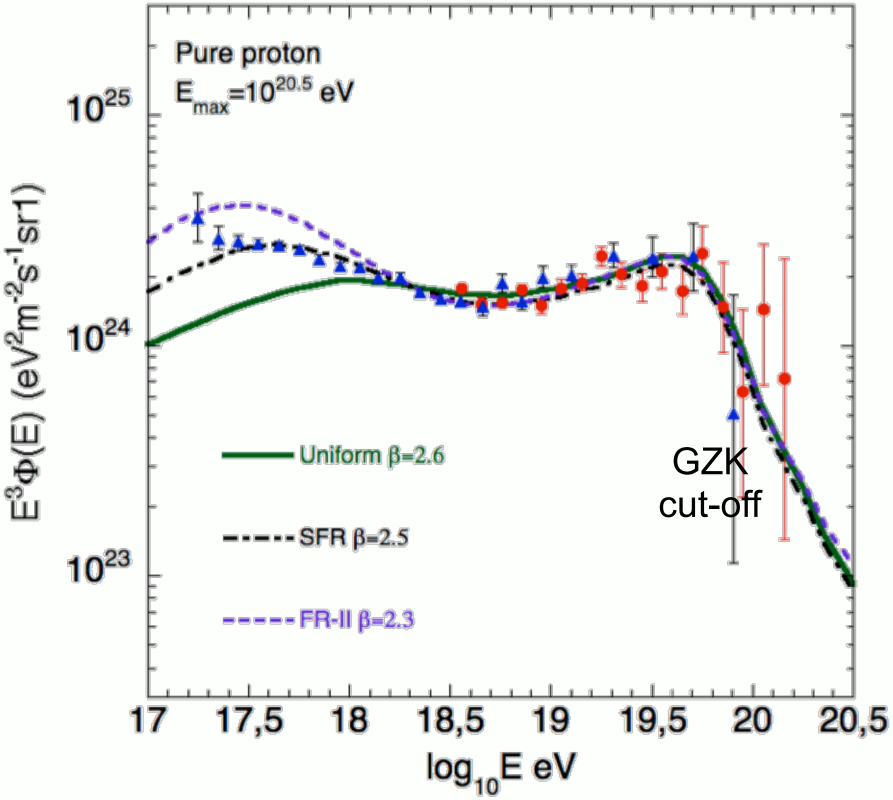

The ankle can be fitted by the extragalactic component itself : pair production dip->the ankle feature has nothing to do with the transition (model developed by Berezinsky et al., 2002-2007)

The GZK attenuation length for nuclei

iron attenuation length

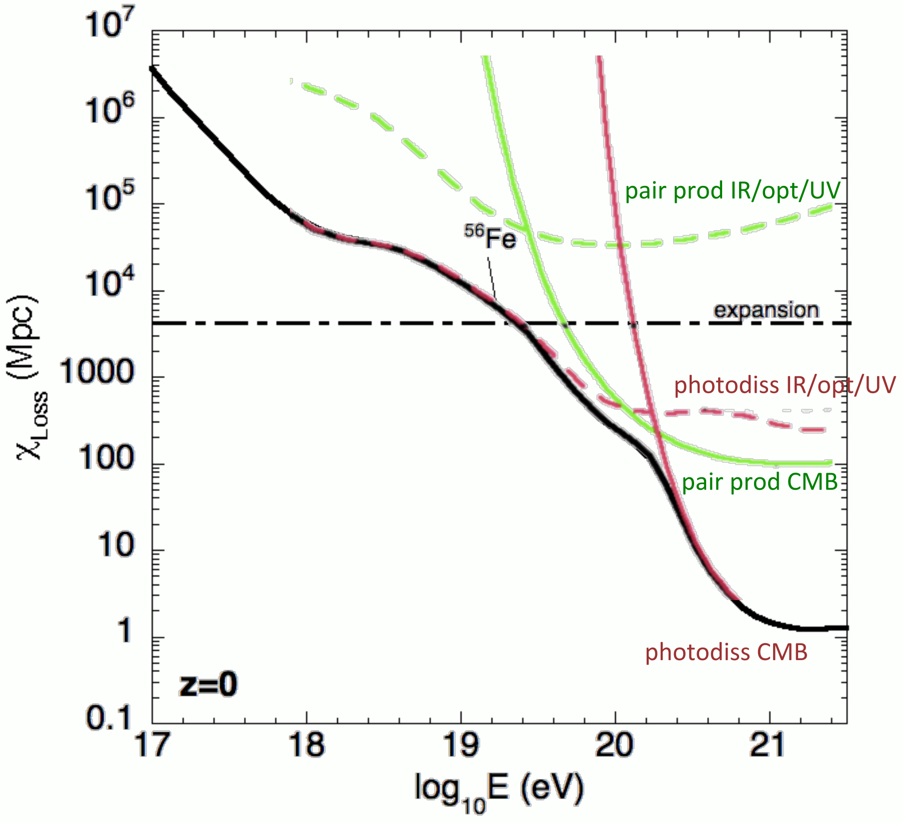

Compound nuclei suffer of:

- Processes triggering a decrease of the Lorentz Factor
    - Adiabatic losses
    - Pair production losses (energy threshold ~A·10^{18} eV)
- Photodisintegration processes
    - Giant Dipole Resonance (GDR); threshold ~ 8 - 20 MeV largest σ and lowest threshold (Khan et al., 2005)
    - Quasi-Deuteron process (QD); threshold ~ 30 MeV
    - Pion production (BR); threshold ~ 145 MeV

The GZK attenuation length for nuclei

nuclei attenuation length

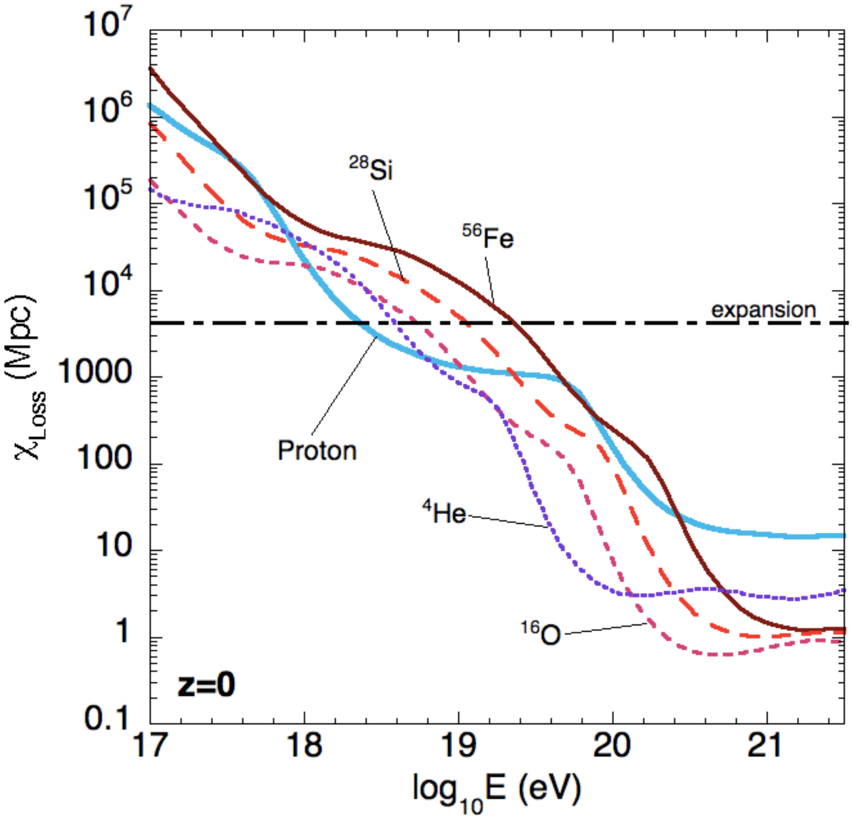

- similar shape of the attenuation length curve for complex nuclei (same processes at play) shifted in energy
- hard to survive above 10^{19} eV for low and intermediate mass nuclei
- different shape for protons (important implications)
- **mostly protons and heavy nuclei expected at the highest energies**

The GZK attenuation length for nuclei

nuclei attenuation length

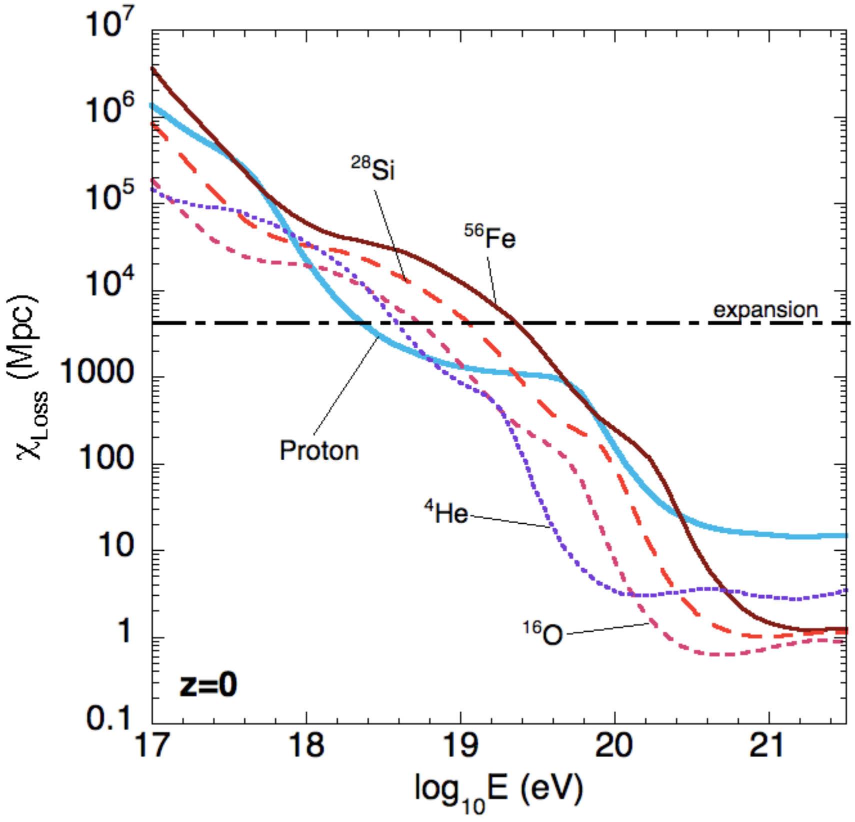

Calculation of the propagated spectrum (Allard 2005)

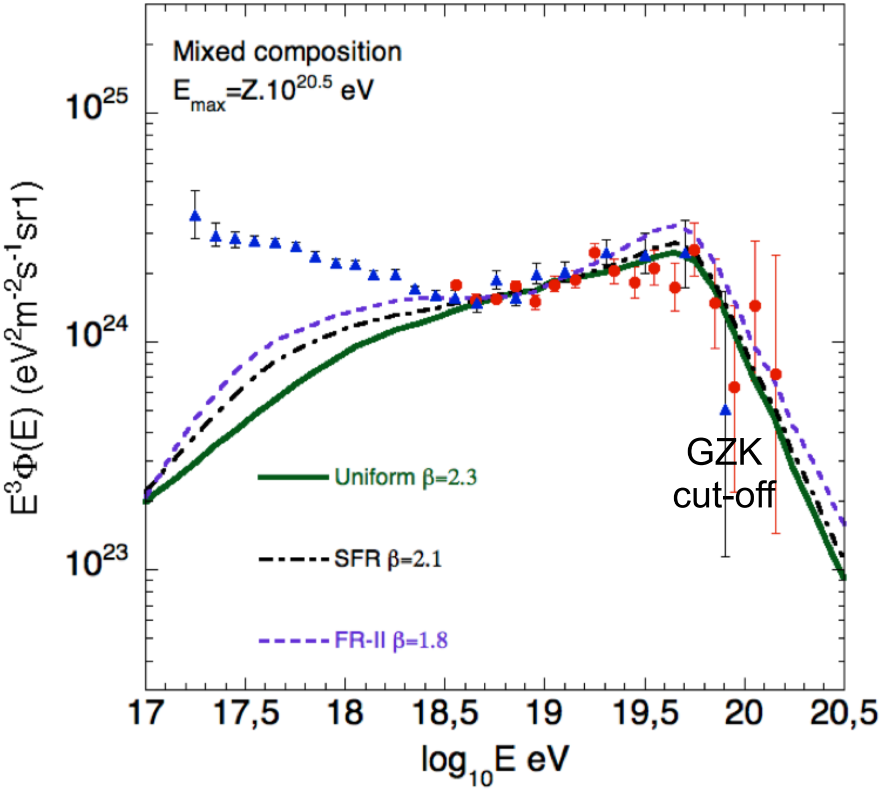

No pair production dip with a mixed composition

The GZK attenuation length for nuclei

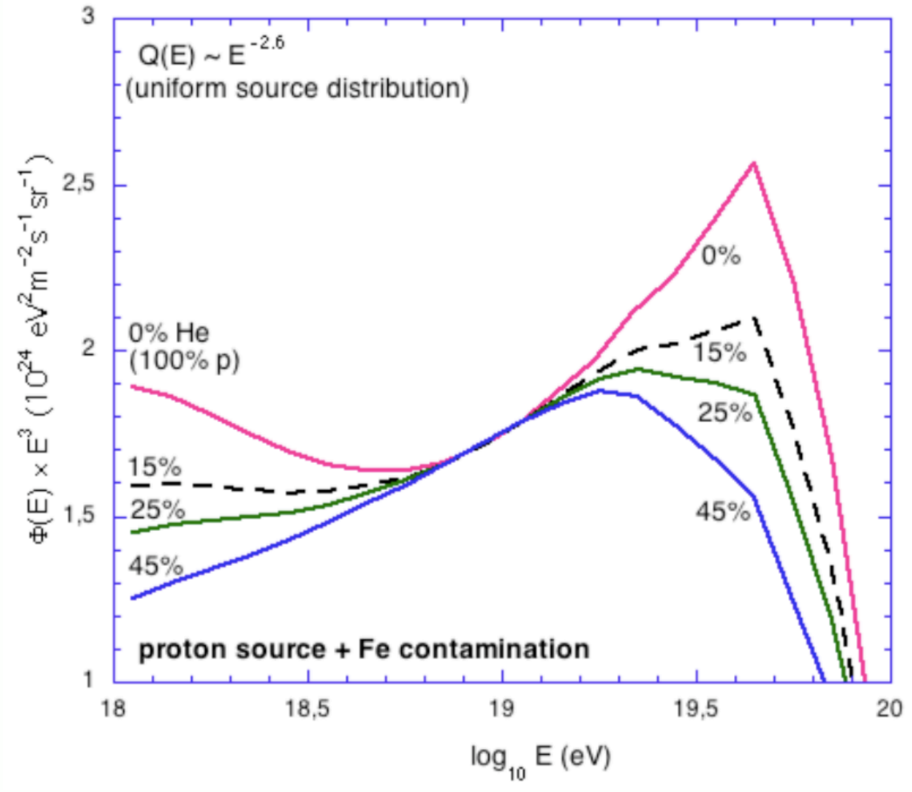

Calculation of the propagated spectrum
(Allard 2005)

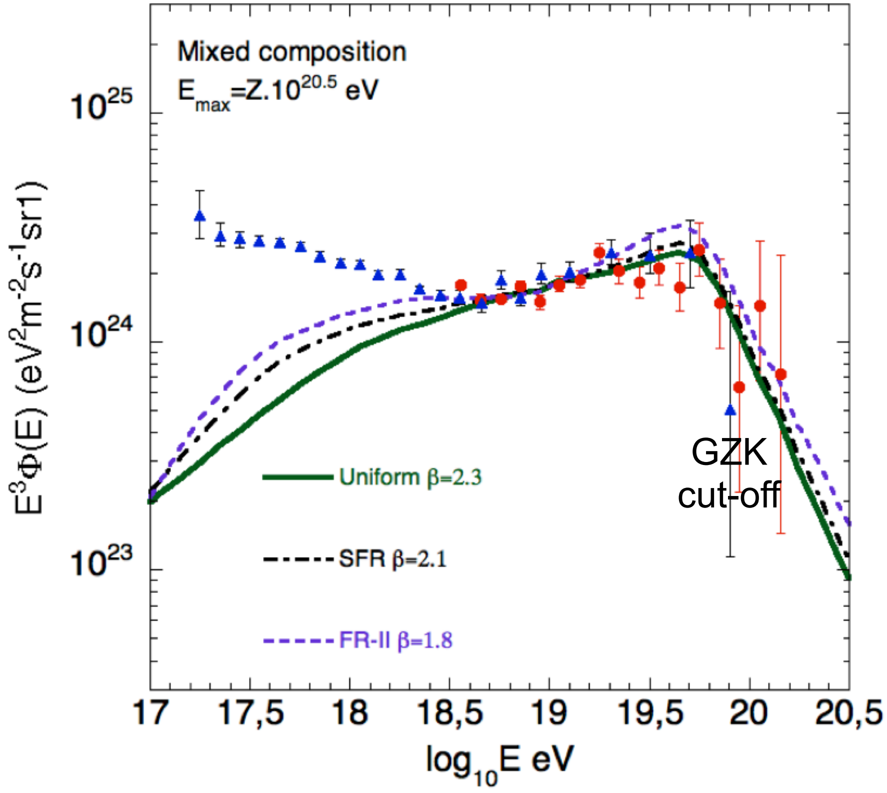

No pair production dip with a mixed composition

A small admixture of nuclei erase the dip !

The ankle is interpreted as the signature of the GCR/EGCR transition

Cosmic Rays primary observables

Energy spectrum

Differential flux

Mass spectrum

composition

Angular spectrum

Arrival direction

Situation at ultra high energy : recent results of PAO

ICRC 2015

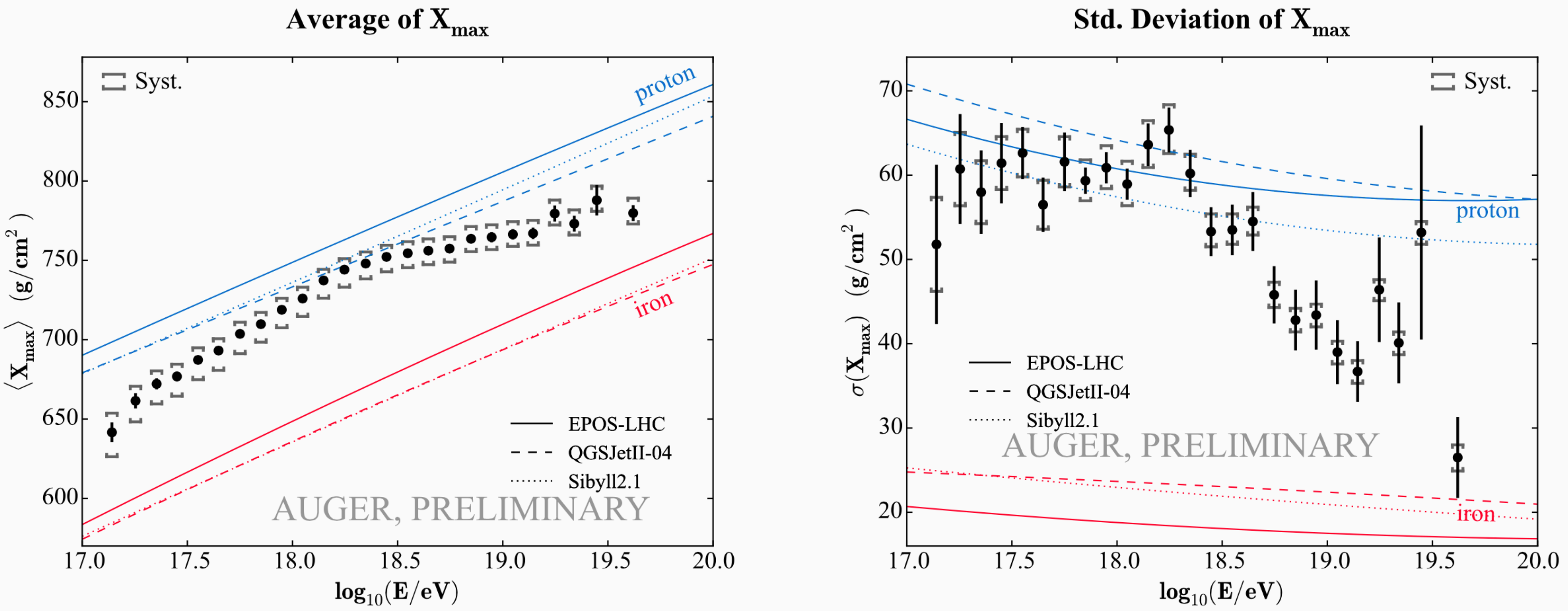

transition towards a heavier composition

-> some care is needed however regarding the uncertainties on the modeling of high energy hadronic interactions

-> Auger is incompatible with the pure proton scenario, TA is compatible with both scenarios (?)

Cosmic Rays primary observables

Energy spectrum → Differential flux

Mass spectrum → composition

Angular spectrum → Arrival direction

The magnetic fog seems to dissipate in the North

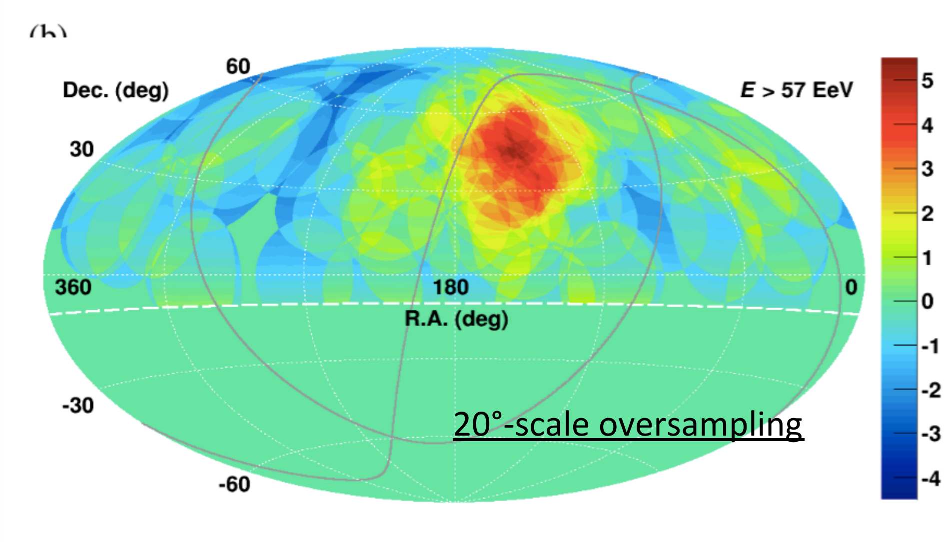

20°-scale oversampling

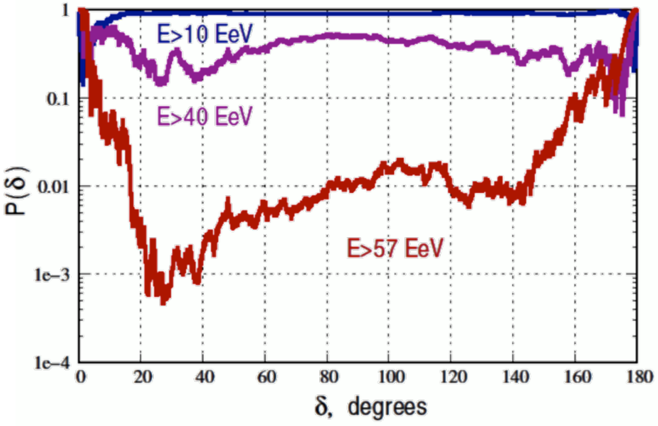

For each angular bin:

1. Count number of pairs of events at in the bin at separation δ
2. Chance Probability is given by the fraction of isotropic MC sets (with equal statistics) with as many or more than the number of pairs seen in data

Compatible with isotropy at E > 10 EeV and E > 40 EeV,
Tension with isotropy at E>57 EeV

6 years of data

87 above 57 EeV (Hot Spot data set)

5.55σ (unpenalized)

7 years of data

83 above 57 EeV (Anisotropy data set)

3.4σ (2pt correlation function)

"The highest-energy set with *E* > 57 EeV demonstrates moderate deviations in all the tests, which are manifestations of the "hot spot" in the distribution of the events — a concentration of the events of the radius ~ 20◦ in the direction R.A. = 148.4◦, Dec. = 44.5◦ (equatorial coordinates). ***The post-trial significance of the hot spot in the 7-year data set is 3.4σ, the same as in the 5-year data set".***

Are the UHECR northern sky and southern sky significantly different ?

TA: 83 above 57 EeV (**TA Anisotropy Data Set)** , exposure 8,600 km^2 sr yr.
After conservatively scaling down the energy by 13%, this corresponds to **83 above 50 EeV.**

Auger: 231 above 52 EeV, exposure 66,452 km^2 sr yr.
Given the shape of the spectrum between 50 and 60 EeV, this extrapolates to ~**290 above 50 EeV**.

If the Auger flux is assumed to represent the average UHECR flux in the absence of anisotropy, then the expected number of events for TA is ~ 38. The actual integrated flux of TA would thus need to be a 7σ upward fluctuation.

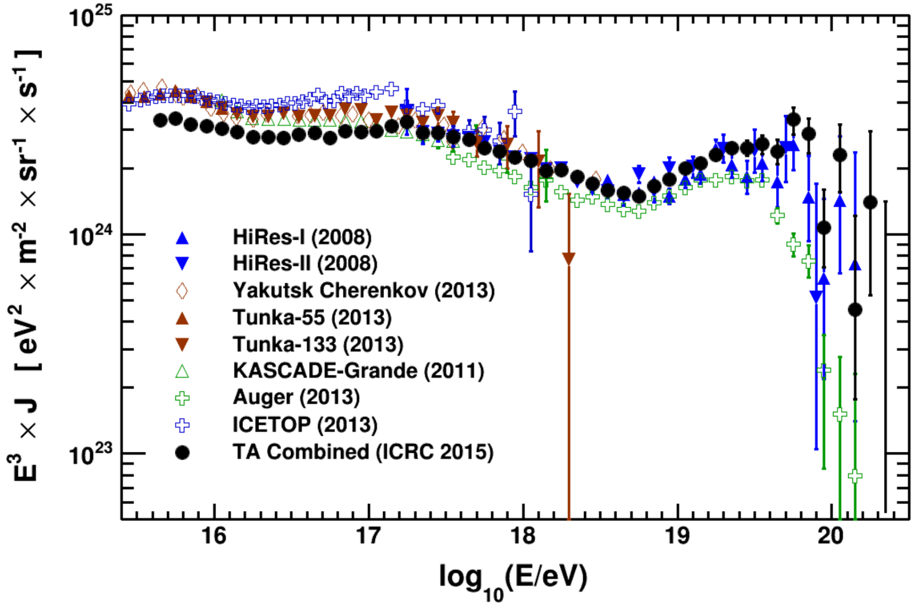

If the difference between the two spectra is taken seriously and attributed to the contribution of a dominant source, this source may represent 45%–60% of the total northern sky flux.

1. Bursting source model

Could UHECRs originate from GRBs?

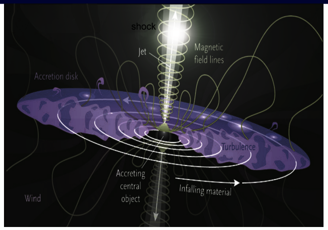

- Gamma-ray bursts (GRBs) are among the best candidate sources for UHECRs (Levinson & Eichler 1993; Milgrom & Usov 1995; Vietri 1995; Waxman 1995...)

- Acceleration in **external shocks** : Vietri 1995, see however Gallant & Achterberg 1999 and recent other works by Niemiec et al. 2006, Niemiec & Ostrowski 2006, Lemoine, Pelletier & Revenu 2006
=> These studies have demonstrated the ineffectiveness of Fermi process in ultra-relativistic shocks

- Acceleration in **internal shocks**: Pioneer work by Waxman 1995, contributions by many other authors/groups : Waxman and collaborators, Dermer and collaborators, Giallis & Pelletier (2003-2005), …

- Gialis & Pelletier (2003) showed that making the assumption of an acceleration time evolving with the energy, which is different from the traditional assumption of Bohm diffusion, can jeopardize the acceleration of particles to the highest energies observed by Auger

- Acceleration of nuclei : Wang et. al (2008), Murase et. al (2008), Metzger et. al (2011) (nucleosynthesis)

- Survival of nuclei in jets : Horiuchi et. al (2012)

- Multimessenger consequences of UHECR acceleration :
  - Photons : Asano & Inoue (2007), Razzaque et al. (2010), Asano et. al (2009), Murase et. al, (2012)
  - Neutrinos : Eichler (1994), Waxman and Bahcall (1997), Guetta et al. (2004), Ahlers et al (2009-2012), Murase and collaborators (2008-2014)

Our calculation

- Modeling of the internal shock according to Daigne & Mochkovitch 1998 ("solid layers" collision model)

$\Longrightarrow$ give us an estimate of the physical quantities at the internal shocks based on a few free parameters

$\Longrightarrow$ prompt emission gamma-ray photons are used as soft photons target for the accelerated cosmic-rays => calculation of the energy losses

- Midly relativistic acceleration of cosmic-rays using the numerical approach of Niemiec & Ostrowski 2004-2006

$\Longrightarrow$ shock parameters are given by the internal shock model

- Full calculation including energy losses (photo-hadron and hadron-hadron)

$\Longrightarrow$ cosmic-ray and neutrino output for a GRB of a given luminosity

- Convolution by a GRB luminosity function and cosmological evolution (Wanderman & Piran 2010)

$\Longrightarrow$ calculation of the diffuse UHECR and neutrino fluxes

$\Longrightarrow$ calculation of composition-dependent observables

$\Longrightarrow$ skymap production

Our calculation

- Modeling of the internal shock according to Daigne & Mochkovitch 1998 (“solid layers” collision model)

⟹ give us an estimate of the physical quantities at the internal shocks based on a few free parameters

⟹ prompt emission gamma-ray photons are used as soft photons target for the accelerated cosmic-rays => calculation of the energy losses

- Midly relativistic acceleration of cosmic-rays using the numerical approach of Niemiec & Ostrowski 2004-2006

⟹ shock parameters are given by the internal shock model

- Full calculation including energy losses (photo-hadron and hadron-hadron)

⟹ cosmic-ray and neutrino output for a GRB of a given luminosity

- Convolution by a GRB luminosity function and cosmological evolution (Wanderman & Piran 2010)

⟹ calculation of the diffuse UHECR and neutrino fluxes
⟹ calculation of composition-dependent observables
⟹ skymap production

Modeling of the internal shock

According to Daigne & Mochkovitch 1998 : a relativistic wind with a varying Lorentz factor is decomposed in discretized solid layers

⇒ Layers collisions mimic the propagation of a shock in the wind

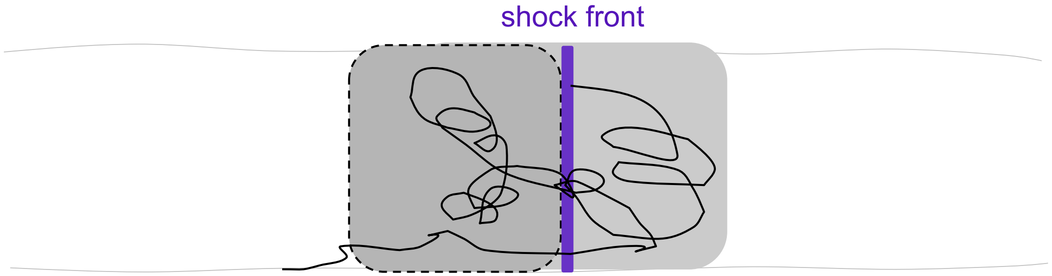

wind free parameters :

wind luminosity L_{wind}, wind duration t_{wind} (in the following we use $t_{wind} = 2$s and $10^{51} < L_{wind} < 10^{55}$ erg.s^{-1})

shock free parameters :

ε_e, ε_B, ε_{CR} equipartition factors for the released energy

Γ_{shock} is given by the relative velocity between 2 colliding layers

Different energy partition models

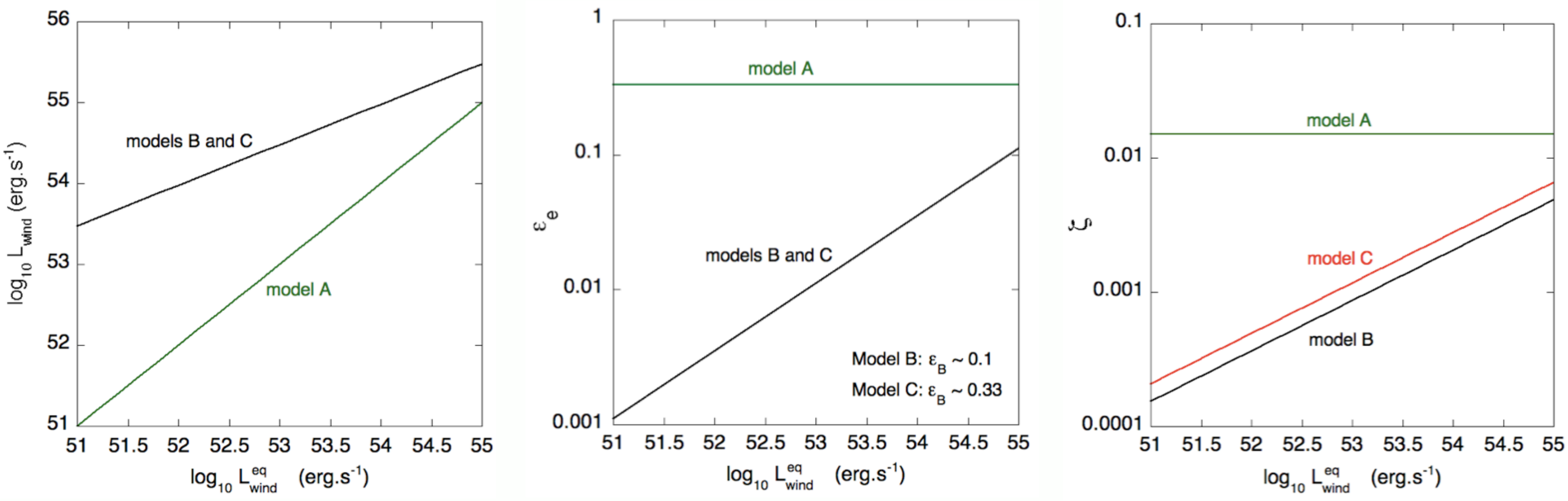

Models B/C: The range of L_{wind} is smaller than what suggested by the prompt emission luminosity function. Fainter GRBs are very inefficient at accelerating electrons but efficient at accelerating CRs

- **Model A: equipartition: ε_e,= ε_B= ε_{CR}= 1/3**
  - Gamma-ray production efficiency ~5% ($L_\gamma \sim L_{wind}/20$)
  - 10^{51} erg/s ≤ L_{wind} ≤ 10^{55} erg/s => 5 10^{49} erg/s ≤ L_γ ≤ 5 10^{53} erg/s (iso)
- **Models B and C: low γ-ray efficiency: ε_e << 1**
  - 3 10^{53} erg/s ≤ L_{wind} ≤ 3 10^{55} erg/s => 5 10^{49} erg/s ≤ L_γ ≤ 5 10^{53} erg/s (iso)
  - Gamma-ray production efficiency: between 0.01% and 1%

Internal shock model: single synthetic pulse

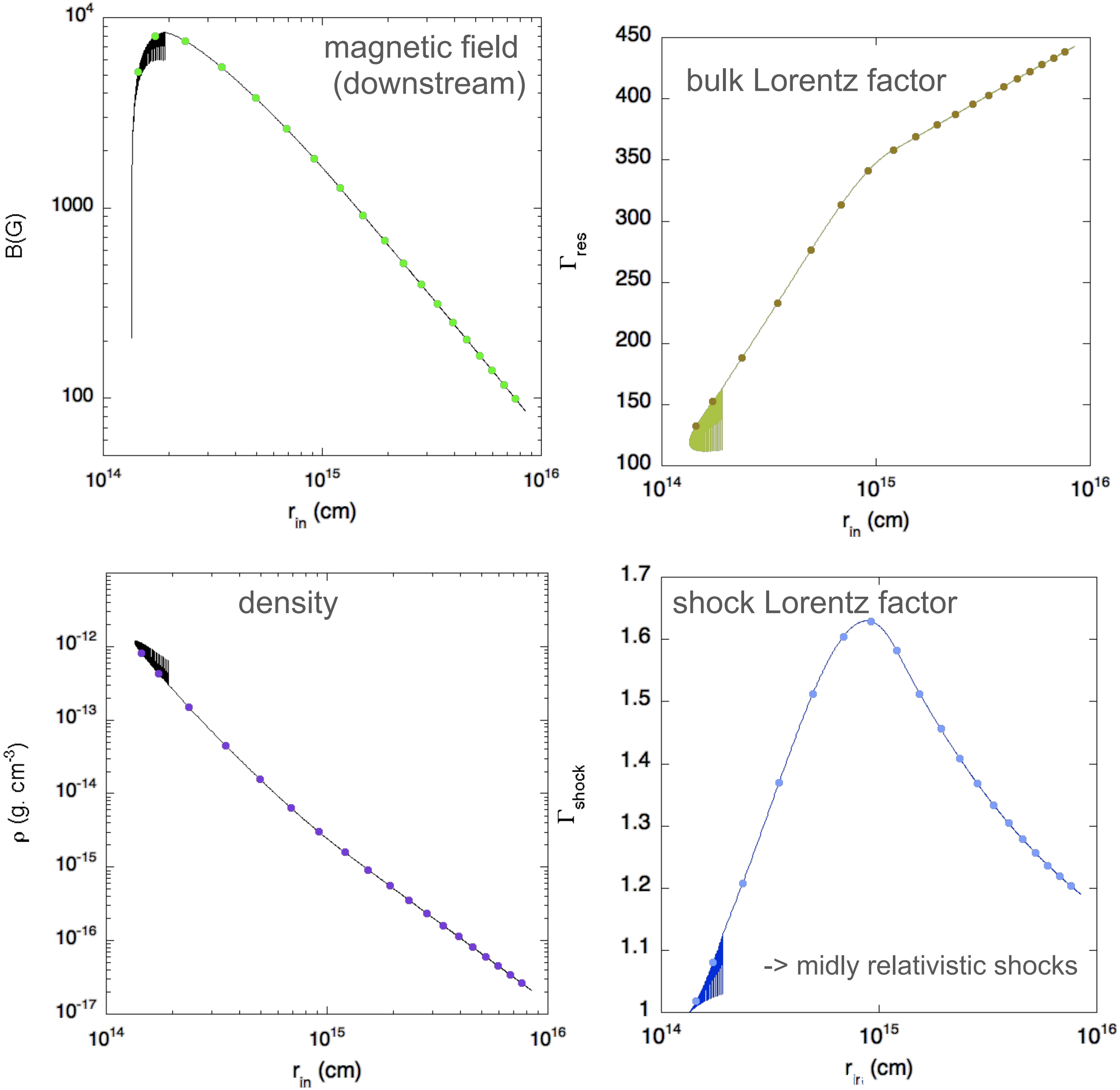

output of this Toy model : physical quantities

...needed for acceleration

B_{rms} (downstream), Γ_{shock}

...needed for energy losses

Γ_{res}, r_{shock},

(needed for adiabatic losses)

$$\frac{1}{E}\frac{dE}{dt} = t_{\rm exp}^{-1} = \frac{\Gamma_{\rm res}\, c}{r_{\rm shock}}$$

+ density, photon background

evolution of a single pulse

$t_{wind} = 2$s
$L_{wind} = 10^{53}$ erg.s^{-1}

18 "snapshots"

output of internal shock model

Energy losses

protons

- pair production 1 MeV

  $p+\gamma \rightarrow p+e^{+}+e^{-}$

- synchrotron emission

  B

- adiabatic losses

  Γ_{res}, r_{shock}

- pion production 150 MeV

  $p+\gamma \rightarrow p \mid n+\Pi^{0} \mid \Pi^{+} \mid \Pi^{-}$

- hadronic interactions density

$$p+p \rightarrow p+n \mid p+\Pi^{0} \mid \Pi^{+} \mid \Pi^{-}$$

$$p+n \rightarrow p+n+\Pi^{0}$$

$$p+n \rightarrow n+n+\Pi^{+}$$

$$p+n \rightarrow p+p+\Pi^{-}$$

complex nuclei $^{A}N_{Z}$

$\Gamma_N \searrow$

OR

$A \searrow$

- GDR 10 MeV
- QD
- BR

QD, BR: pion production 30 - 145 MeV

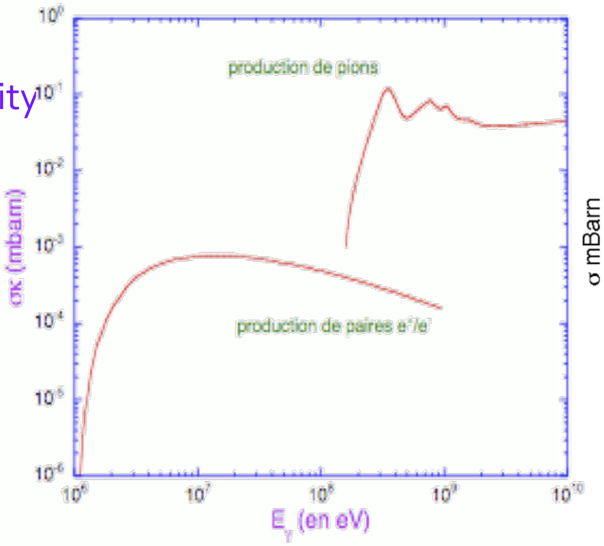

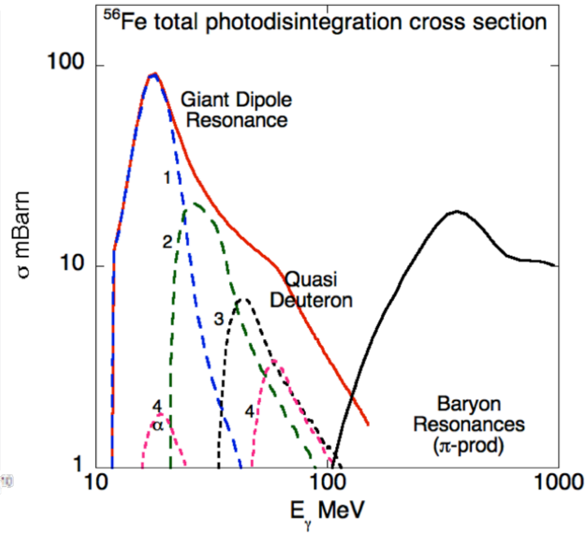

t_{loss} computed with prompt emission SEDs

proton

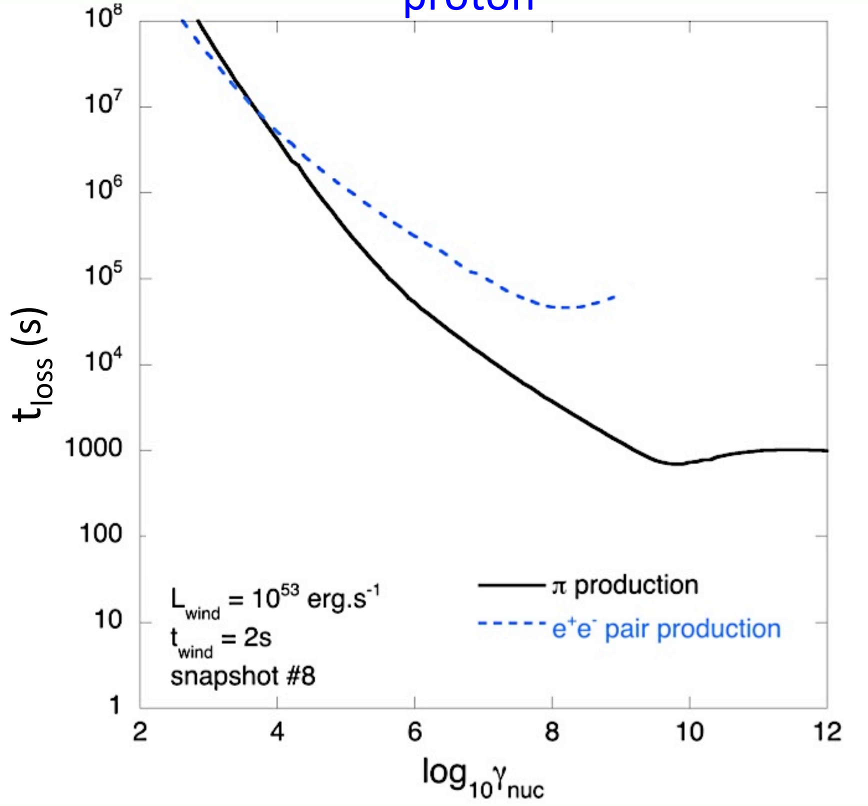

Fe nuclei

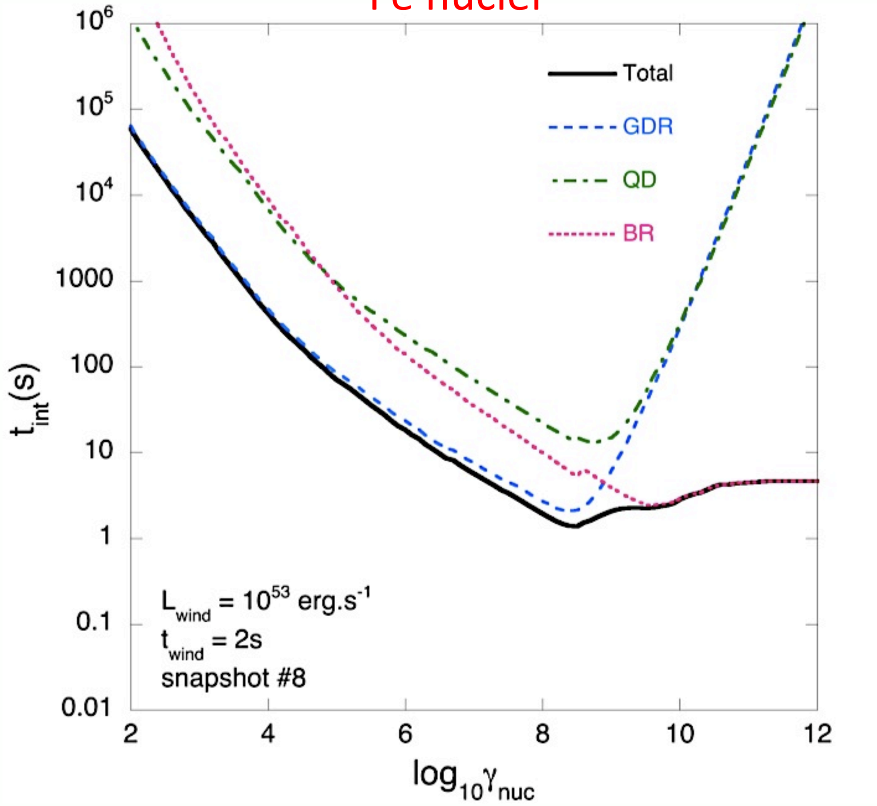

We apply the revised scheme of photo-nuclear interactions described in Khan et al. 2005.

$$\lambda^{-1}_{Band} = \frac{1}{2\gamma^2}\int_{E'_{seuil}/2\gamma}^{E_{max}} \frac{n(E)}{E^2}\left(\int_{E'_{seuil}}^{2\gamma E} E'\sigma(E')dE'\right)dE$$

(see Allard et al., 2005 A&A, 443, 29
for details and Allard, 2012 for a review)

Our calculation

- Modeling of the internal shock according to Daigne & Mochkovitch 1998 (“solid layers” collision model)

⟹ give us an estimate of the physical quantities at the internal shocks based on a few free parameters

⟹ prompt emission gamma-ray photons are used as soft photons target for the accelerated cosmic-rays => calculation of the energy losses

- Midly relativistic acceleration of cosmic-rays using the numerical approach of Niemiec & Ostrowski 2004-2006

⟹ shock parameters are given by the internal shock model

- Full calculation including energy losses (photo-hadron and hadron-hadron)

⟹ cosmic-ray and neutrino output for a GRB of a given luminosity

- Convolution by a GRB luminosity function and cosmological evolution (Wanderman & Piran 2010)

⟹ calculation of the diffuse UHECR and neutrino fluxes

⟹ calculation of composition-dependent observables

⟹ skymap production

Numerical method for CR acceleration at relativistic shock

We follow Niemiec & Ostrowski 2004-2006 method to simulate Fermi cycles at relativistic shocks :
Full calculation of particles trajectories and shock crossing ➔ Fermi cycles

- Needs assumption on the magnetic field configuration upstream
- jump conditions given by Synge 1957 for relativistic shocks

➔ **B** compressed and amplified in the direction perpendicular to the shock normal

- We assume a Kolmogorov-type turbulence uptream in what follows

- Needs assumptions on free boundaries :

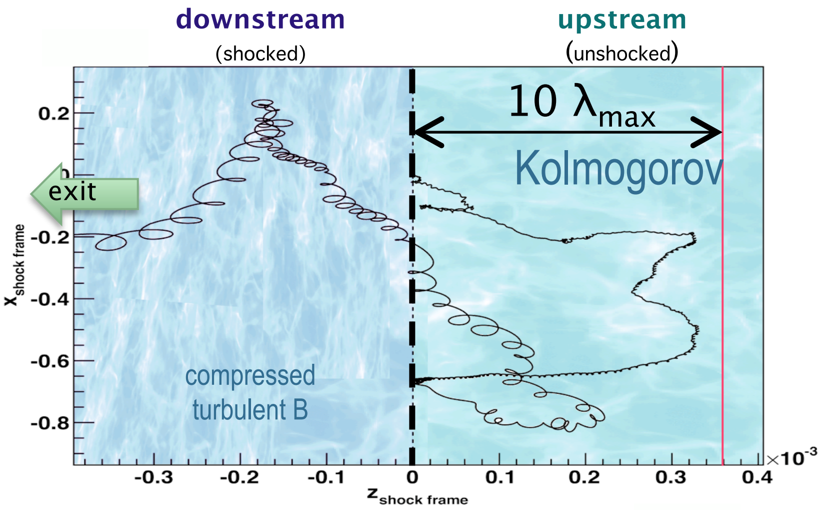

Particle trajectory (3D) in the shock frame
9 cycles before escaping downstream. Energy gain~ 70.

Downstream boundary is set by the comoving width of the shocked medium at a given stage of the shock propagation ➔ Input from F. Daigne hydrodynamical code

Upstream we assume that the turbulence does not extend further than a distance $10\,\lambda_{\text{max}}$ from the shock (λ_{max} is the maximum turbulence scale)

Spectra of accelerated cosmic rays

rigidity $R = \frac{pc}{Ze} \approx \frac{E(eV)}{Z}$

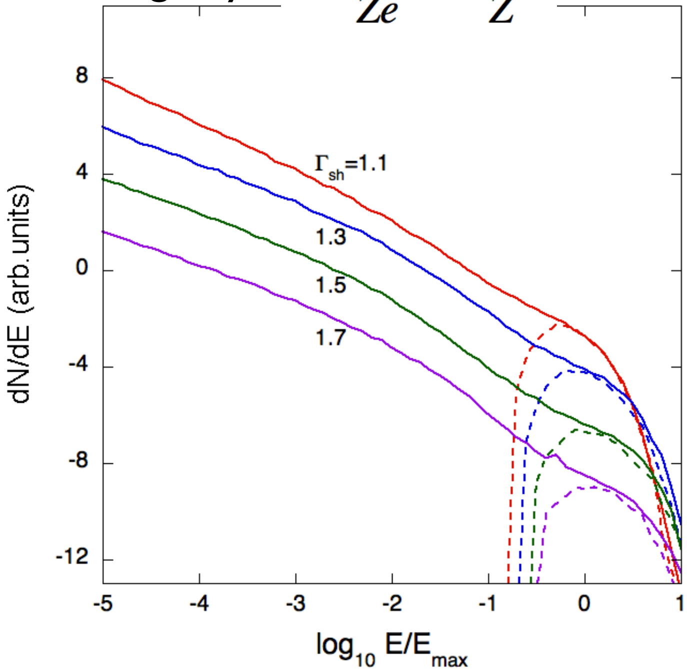

R_{max} definition : $r_L(R_{max}) = \frac{R_{max}}{Bc} = \lambda_{max}$

- Escape upstream : high pass filter (select particles in the weak scattering regime)

- Escape downstream : should become a high pass filter in presence of energy losses (particles must leave fast enough before being cooled by energy losses)

Spectra of accelerated cosmic-rays are never really perfect power law

The shape depends strongly on the magnetic field configuration

Parallel shocks can lead to very hard spectral indexes
Perpendicular shocks can lead to soft spectra with early cut-offs
(results qualitatively identical to those obtained by Niemiec & Ostrowski)

For a complete picture one needs to plug energy losses in

UHECR spectra (escaping from the wind)

We calculate spectra of escaping cosmic-rays for wind luminosities between 10^{51} and 10^{55} erg.s^{-1}

⇒**GRB output for :** **$L\gamma=5.10^{49}$** erg.s^{-1} $t_{wind} = 2$s
metallicity : 10 X galactic CRs

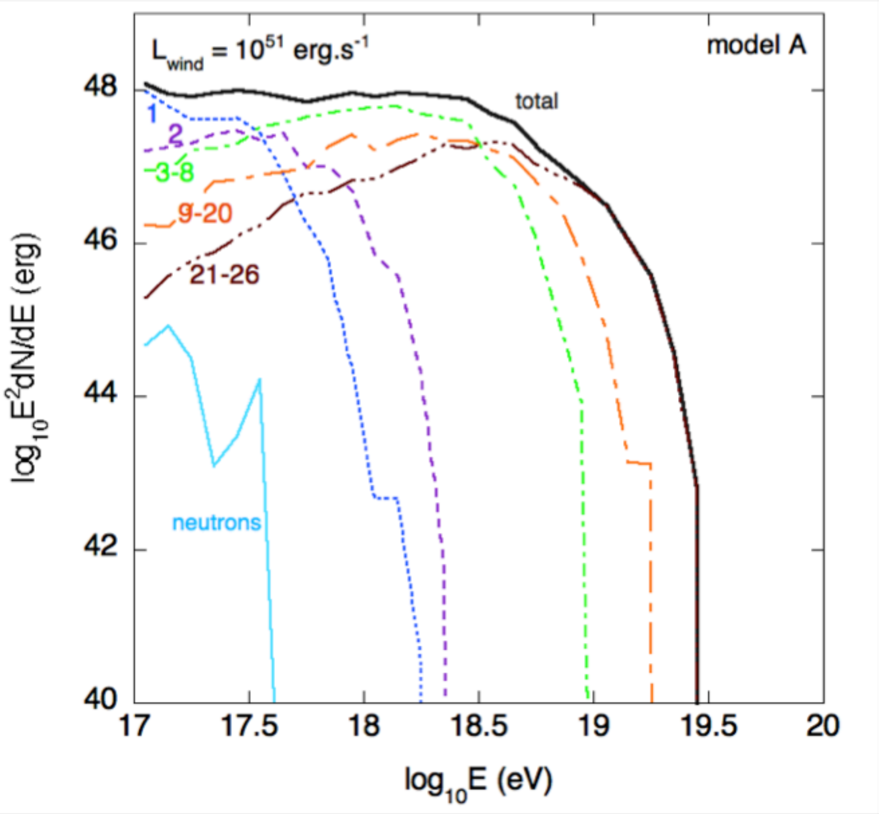

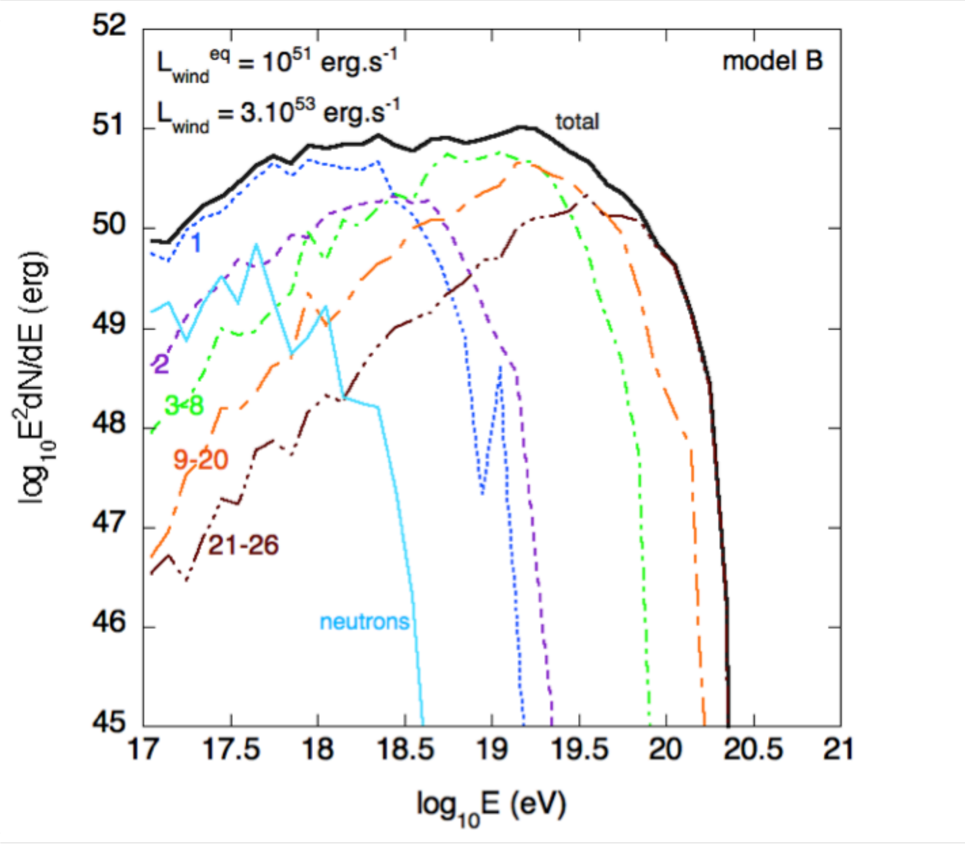

UHECR spectra (escaping from the wind)

We calculate spectra of escaping cosmic-rays for wind luminosities between 10^{51} and 10^{55} erg.s^{-1}

⇒**GRB output for :** **$L\gamma=5.10^{51}$** erg.s^{-1} $t_{wind} = 2$s
metallicity : 10 X galactic CRs

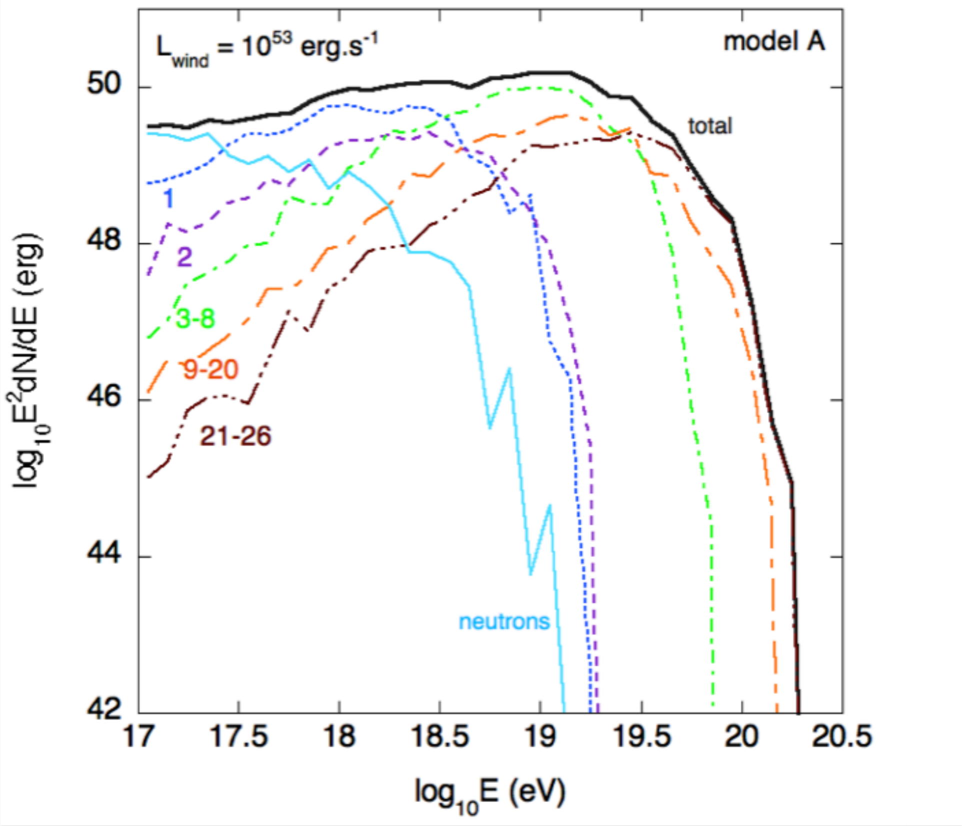

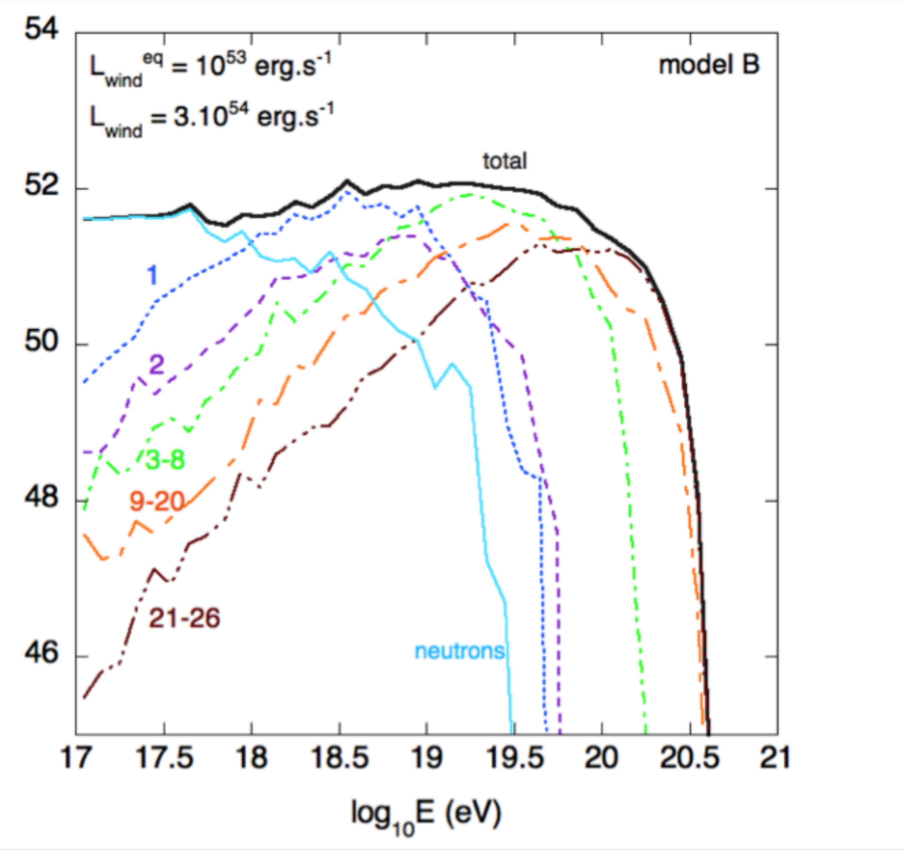

UHECR spectra (escaping from the wind)

We calculate spectra of escaping cosmic-rays for wind luminosities between 10^{51} and 10^{55} erg.s^{-1}

⇒**GRB output for :** **$L\gamma$=5.10^{53}** erg.s^{-1} t_{wind} = 2s
metallicity : 10 X galactic CRs

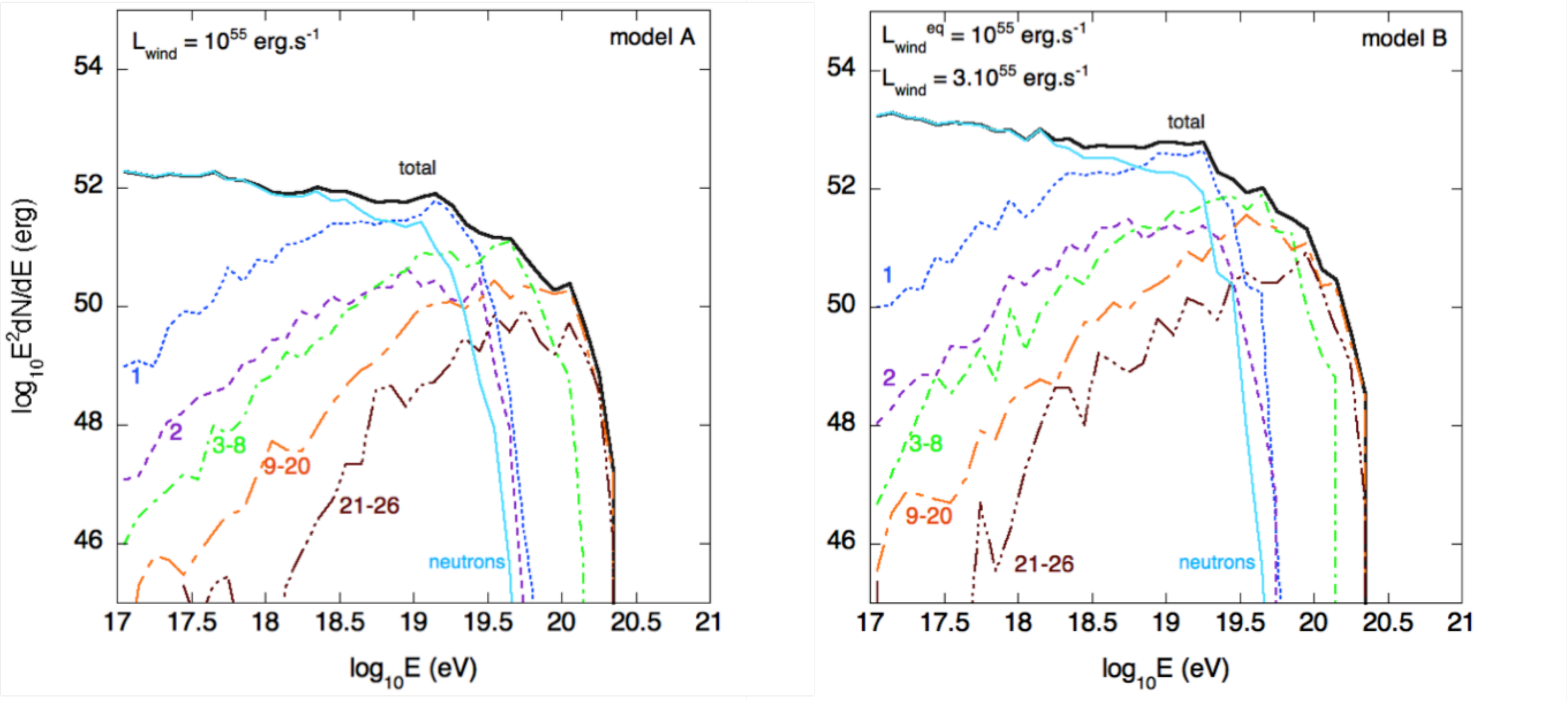

High luminosities : Nuclei components get narrower, more neutrons emitted
➔ photointeractions of nuclei

Our calculation

- Modeling of the internal shock according to Daigne & Mochkovitch 1998 (“solid layers” collision model)

$\Longrightarrow$ give us an estimate of the physical quantities at the internal shocks based on a few free parameters

$\Longrightarrow$ prompt emission gamma-ray photons are used as soft photons target for the accelerated cosmic-rays => calculation of the energy losses

- Midly relativistic acceleration of cosmic-rays using the numerical approach of Niemiec & Ostrowski 2004-2006

$\Longrightarrow$ shock parameters are given by the internal shock model

- Full calculation including energy losses (photo-hadron and hadron-hadron)

$\Longrightarrow$ cosmic-ray and neutrino output for a GRB of a given luminosity

- Convolution by a GRB luminosity function and cosmological evolution (Wanderman & Piran 2010)

$\Longrightarrow$ calculation of the diffuse UHECR and neutrino fluxes

$\Longrightarrow$ calculation of composition-dependent observables

$\Longrightarrow$ skymap production

Modeling the Cosmic Rays primary observables

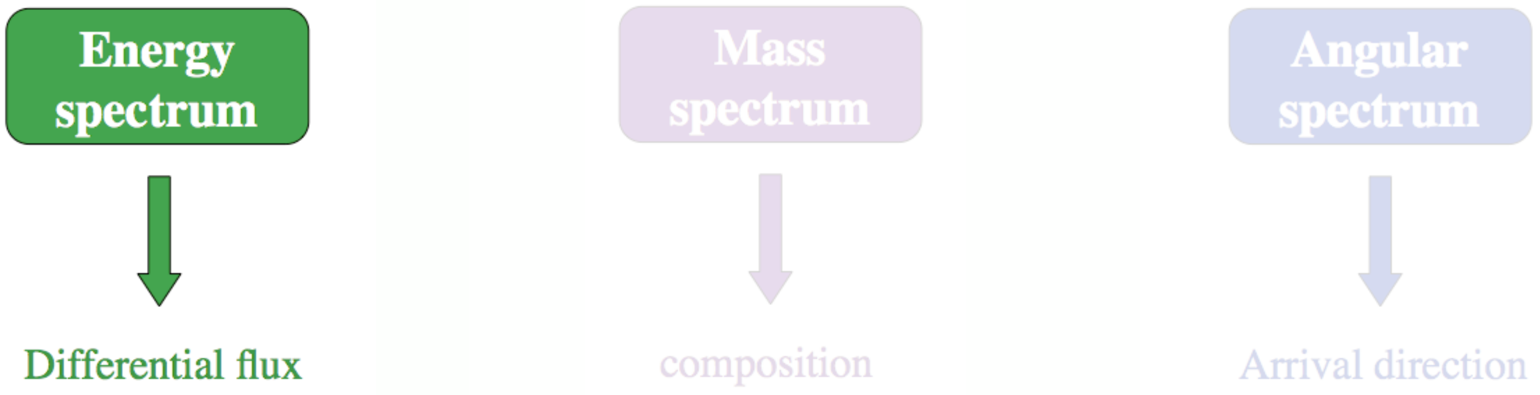

Energy spectrum → Differential flux

Mass spectrum → composition

Angular spectrum → Arrival direction

Resulting UHECR propagated spectrum

- Implement the GRB rate, GRB luminosity function, and redshift evolution from Wanderman & Piran (2010)

$$\frac{dN_{\mathrm{GRB}}}{dL_\gamma}(L_\gamma) \propto \begin{cases} L_\gamma^{-\alpha} & \text{for } L_\gamma \leqslant L_\star \\ L_\gamma^{-\beta} & \text{for } L_\gamma > L_\star \end{cases}$$

$\alpha = 1.2$
$\beta = 2.4$

$$\rho_{GRB}(z) = \rho_{GRB}(0) \times \begin{cases} (1+z)^{n_1} & \text{for } z \leqslant z_\star \\ (1+z_\star)^{n_1-n_2} \times (1+z)^{n_2} & \text{for } z > z_\star \end{cases}$$

$$\rho_{\mathrm{GRB}}(0) = 1.3\,\mathrm{Gpc}^{-3}\,\mathrm{yr}^{-1}$$

$n_1 = 2.1$
$n_2 = -1.4$
$z_* = 3$

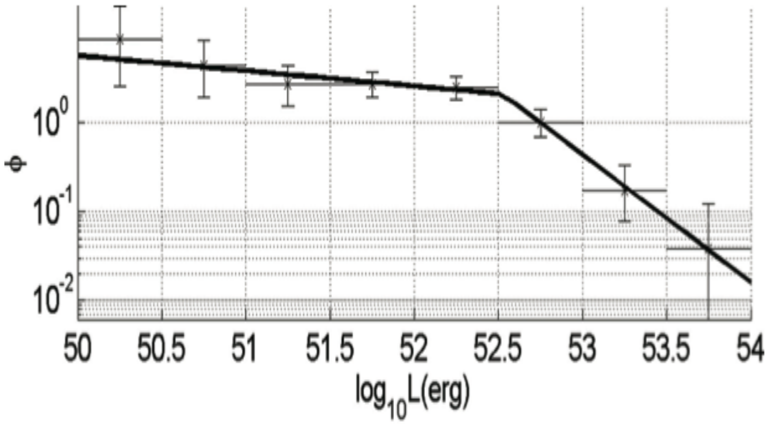

Assuming the central source activity lasts 20s

UHECR emissivity above 10^{18} eV :

Model A : ~6.10^{42} erg.Mpc^{-3}.yr^{-1}

Model B and C : ~3–4.10^{44} erg.Mpc^{-3}.yr^{-1}

One would need a few 10^{44} erg.Mpc^{-3}.yr^{-1}
above 10^{18} eV to reproduce the UHECR data

Resulting UHECR propagated spectrum

300 realisations of the history of GRB explosions in the Universe

Propagation in extragalactic turbulent magnetic field, including energy losses on extragalactic photon backgrounds (see Globus, Allard & Parizot 2008 for details)

- **Cosmological Microwave Background**, very well known T=2.726K

⇒ trivial cosmological evolution $\lambda(E,z)=\lambda(E(1+z),z=0)/(1+z)^3$

- **Infra-red, optical, ultra-violet backgrounds (IR/OPT/UV)**

Time evolution dependent on the Star Formation Rate, stars aging and metalicity (especially the UV background)

⇒ non trivial but recently better constrained by astrophysical data (Spitzer telescope, etc…)

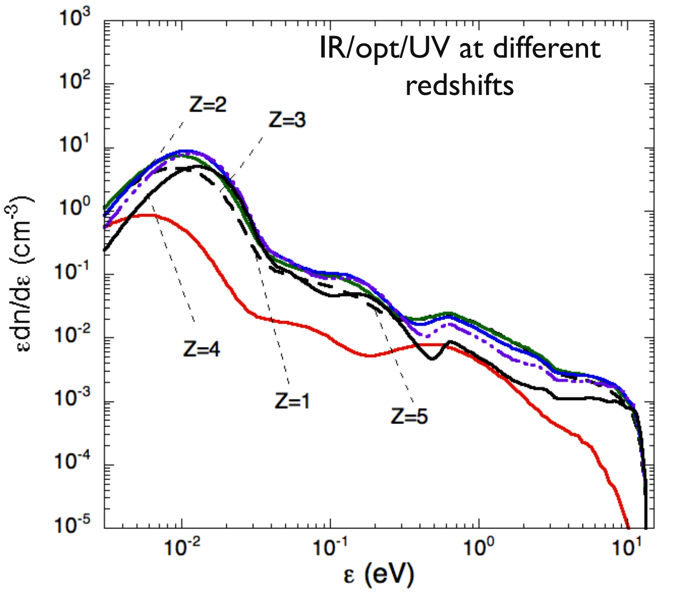

In the following calculations, we use estimate of IR/OPT/UV background density and time evolution from Kneiske et al., 2006

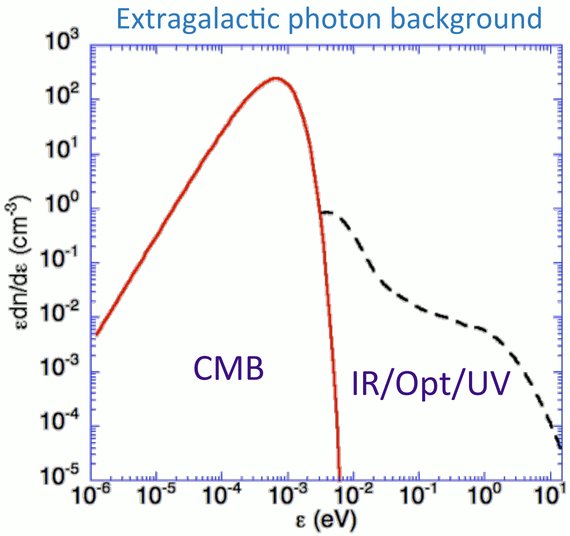

Resulting UHECR propagated spectrum

Assumptions
ϵ_e = 0.33
ϵ_B = 0.33
ϵ_{CR} = 0.33
ξ_e = 0.01

Model A = equipartition

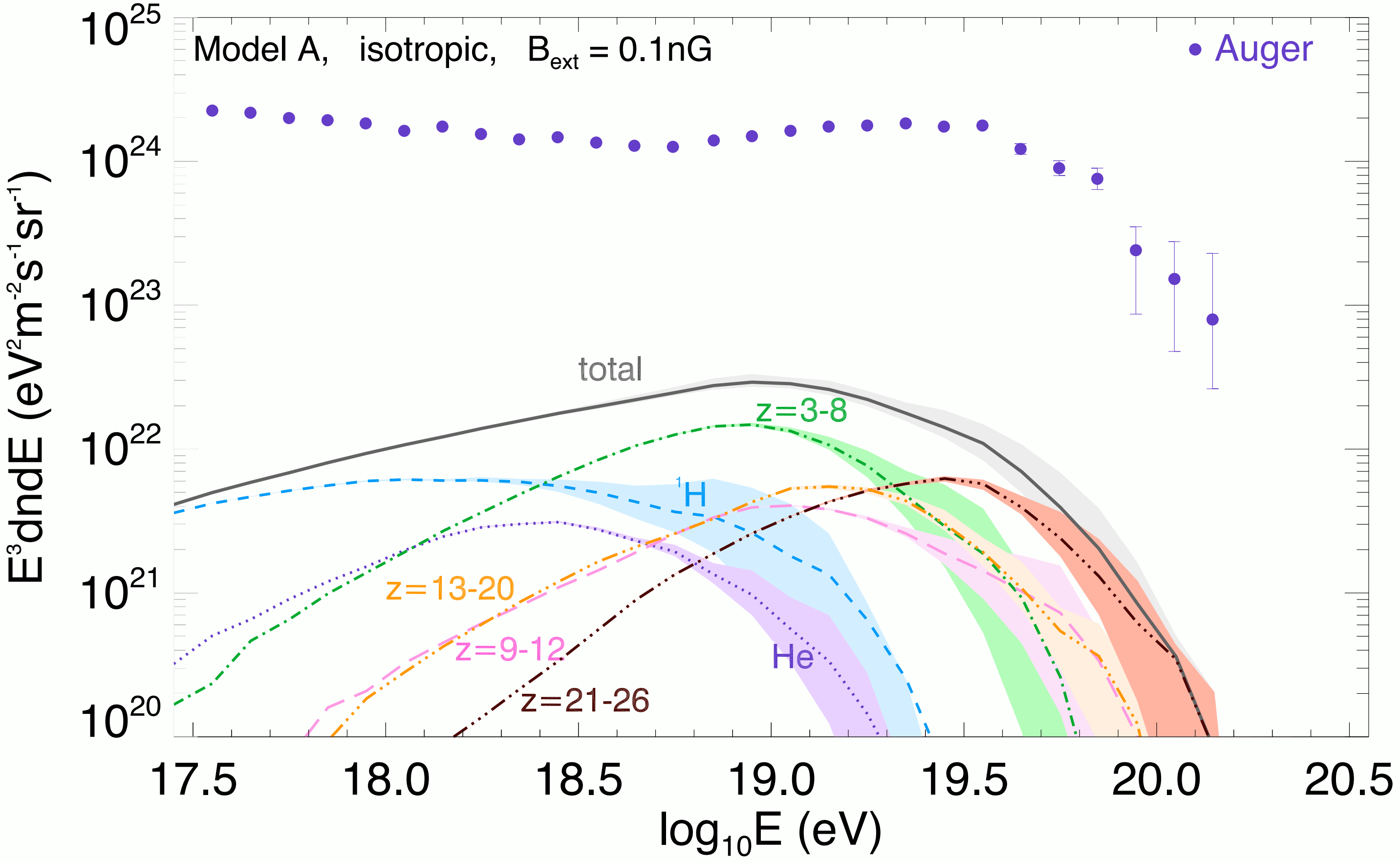

300 realisations of the history of GRB explosions in the Universe

Resulting UHECR propagated spectrum

Assumptions

ε_e << 1

ε_B ~ 0.1

ε_{CR} ~ 0.9

ξ_e << 1

Model B/C = low γ-ray efficiency

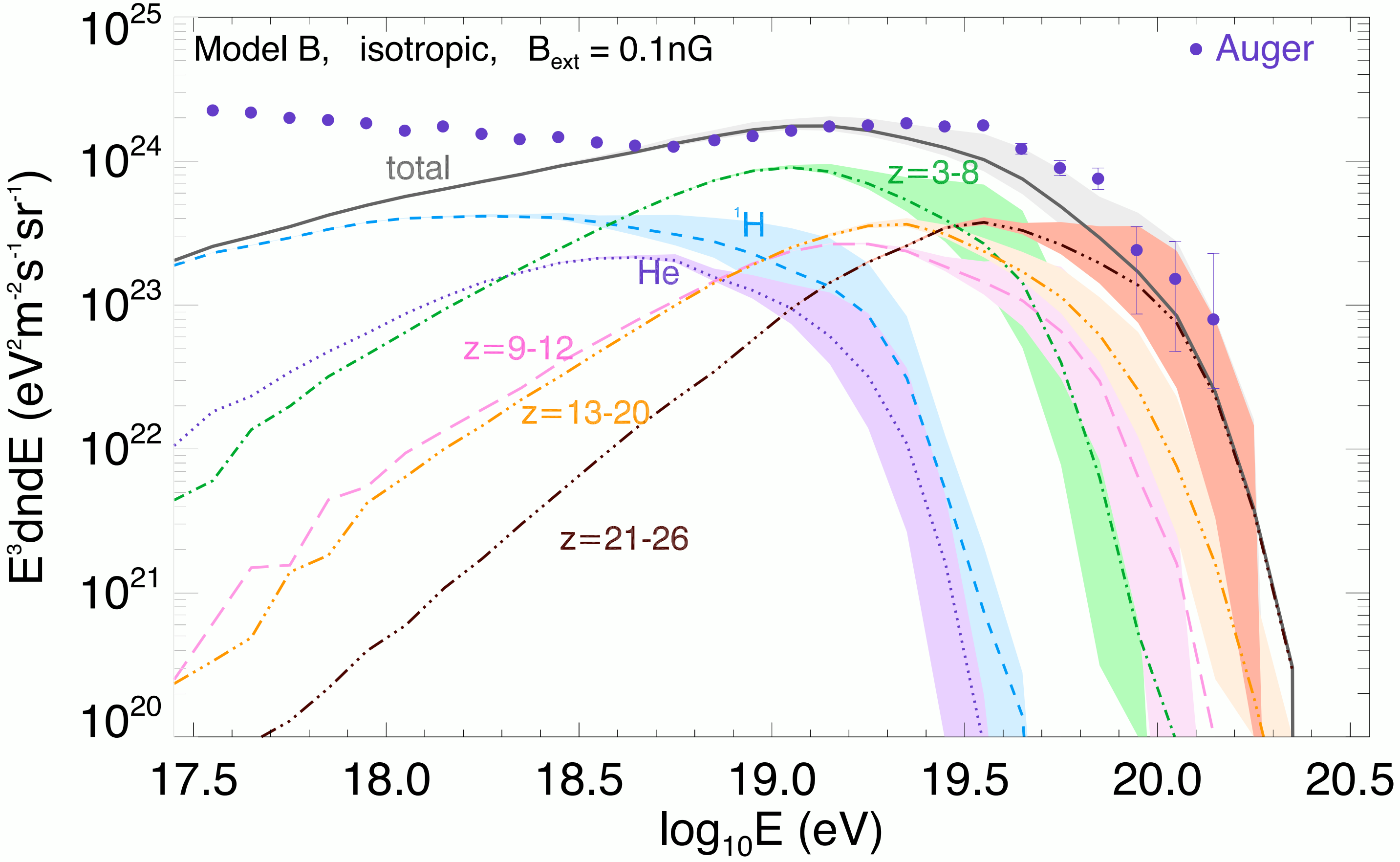

300 realisations of the history of GRB explosions in the Universe

Resulting UHECR propagated spectrum

Assumptions

ε_e << 1

ε_B ~ 0.5

ε_{CR} ~ 0.5

ξ_e << 1

Model B/C = low γ-ray efficiency

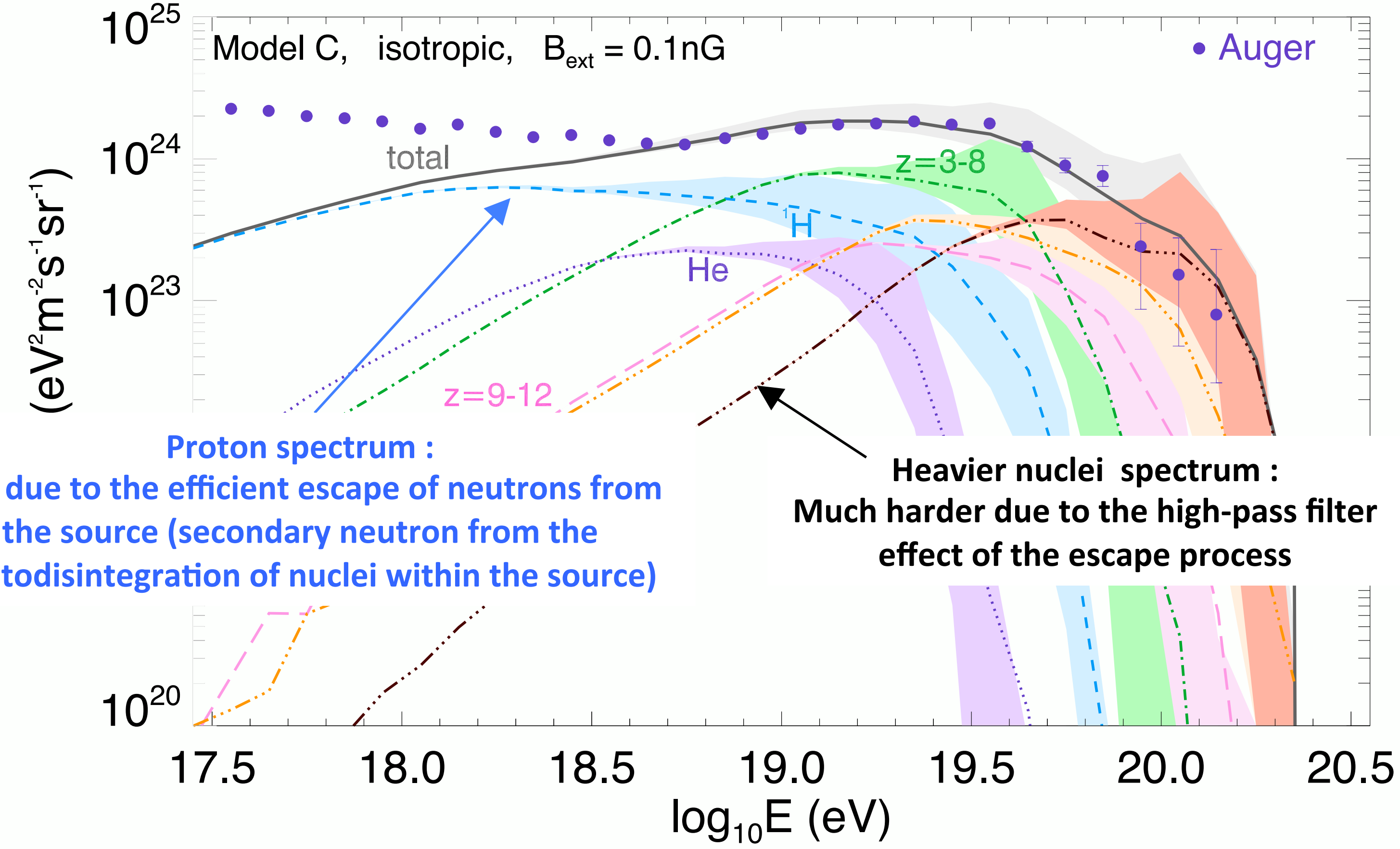

Proton spectrum :
Soft due to the efficient escape of neutrons from the source (secondary neutron from the photodisintegration of nuclei within the source)

Heavier nuclei spectrum :
Much harder due to the high-pass filter effect of the escape process

N. Globus, D. Allard, R. Mochkovitch, E. Parizot, MNRAS, 2015

Resulting UHECR propagated spectrum

Assumptions
ε_e << 1
ε_B ~ 0.5
ε_{CR} ~ 0.5
ξ_e << 1

Model B/C = low γ-ray efficiency

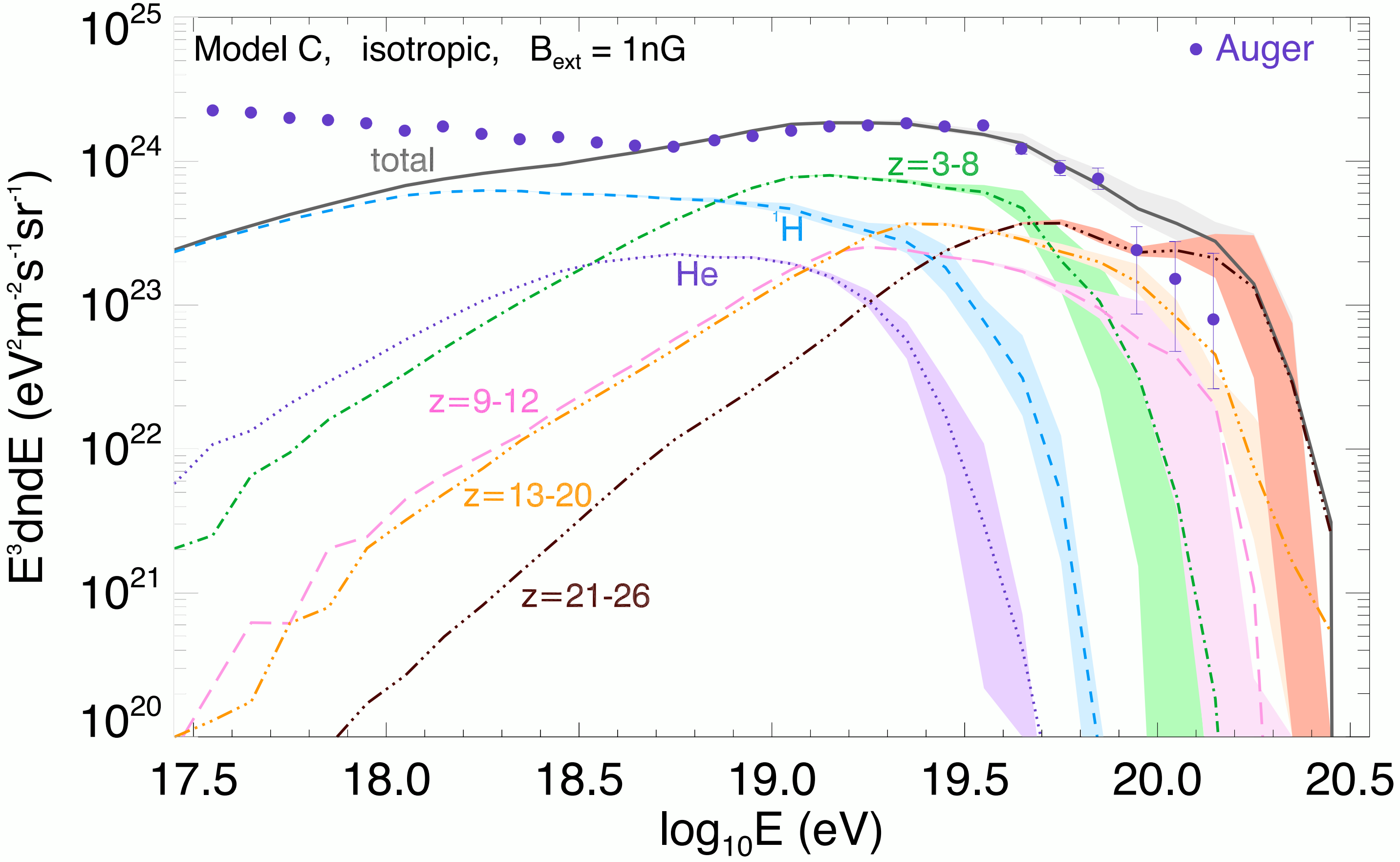

N. Globus, D. Allard, R. Mochkovitch, E. Parizot, MNRAS, 2015

Modeling the Cosmic Rays primary observables

Energy spectrum

Differential flux

Mass spectrum

composition

Angular spectrum

Arrival direction

Resulting UHECR composition

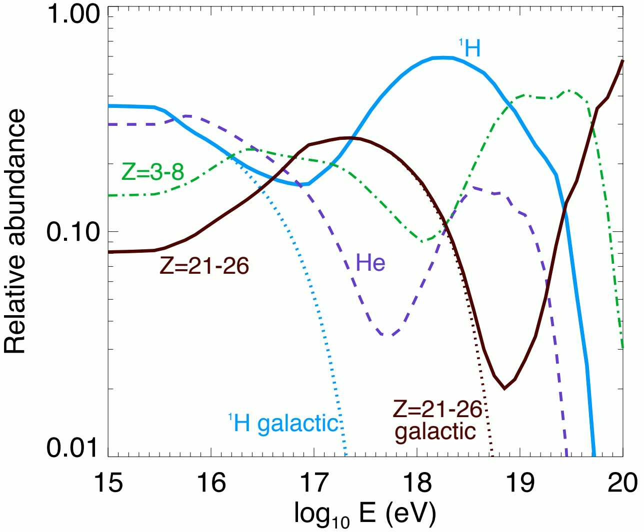

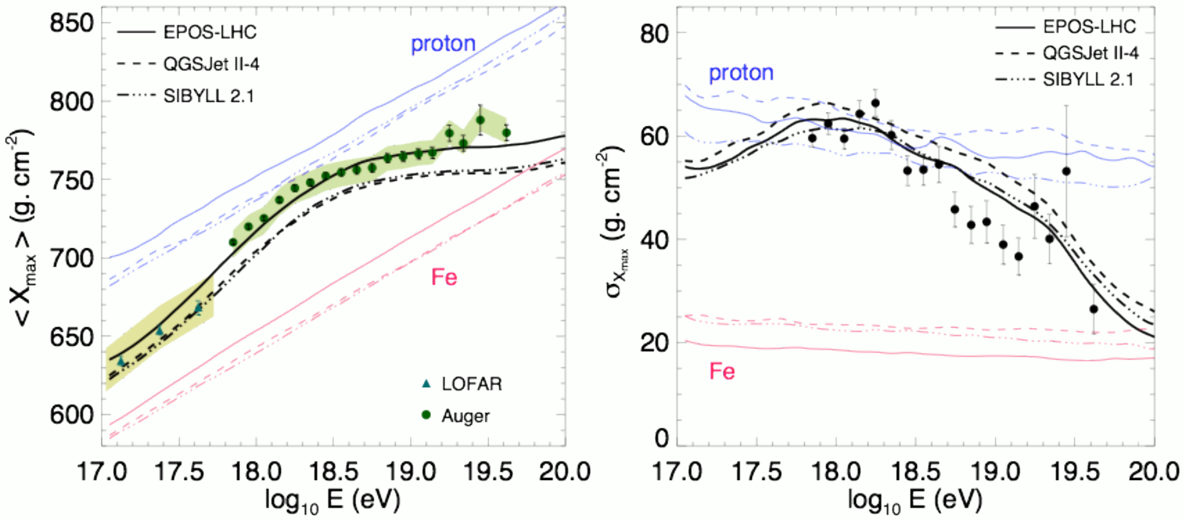

⟹ **The model provides a good description of the evolution of the composition (Auger, LOFAR)**

Prediction: the dominant class of nuclei between ~6 10^{18} eV and ~5 10^{19} eV should be CNO

⟹ **GRB Internal shocks are good particle accelerators (protons up to few 10^{19} eV, iron to 10^{20} eV) but extragalactic GRBs as sources of UHECRs are excluded if one assumes equipartition**

⟹ **Due to neutrons escape UHE protons injected into the extragalactic medium have a much softer spectrum than UHE nuclei**

NB: this is a generic feature of acceleration models in high radiation density environment and a key feature for the ankle transition

Recent Kascade-Grande analyses

The heavy knee and the light ankle
$E \sim 10^{17}$ eV

KG showed evidence for an "ankle" in the light component

KG collab, PHYSICAL REVIEW D 87, 081101(R) (2013)

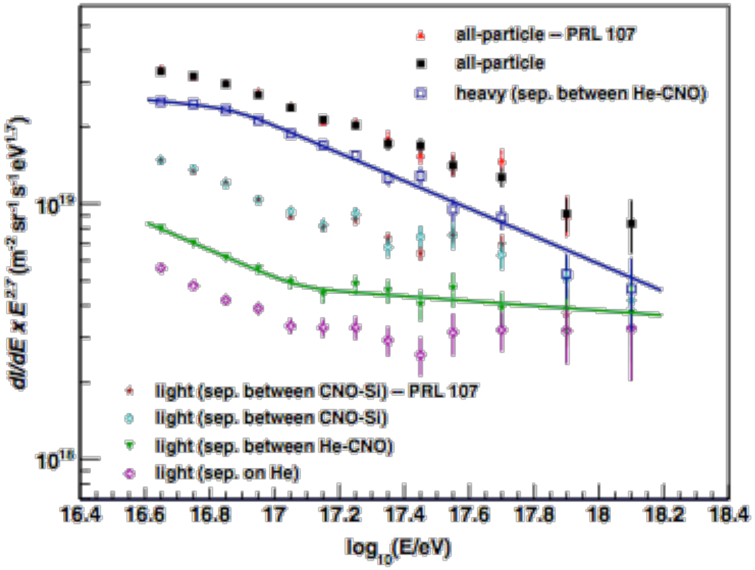

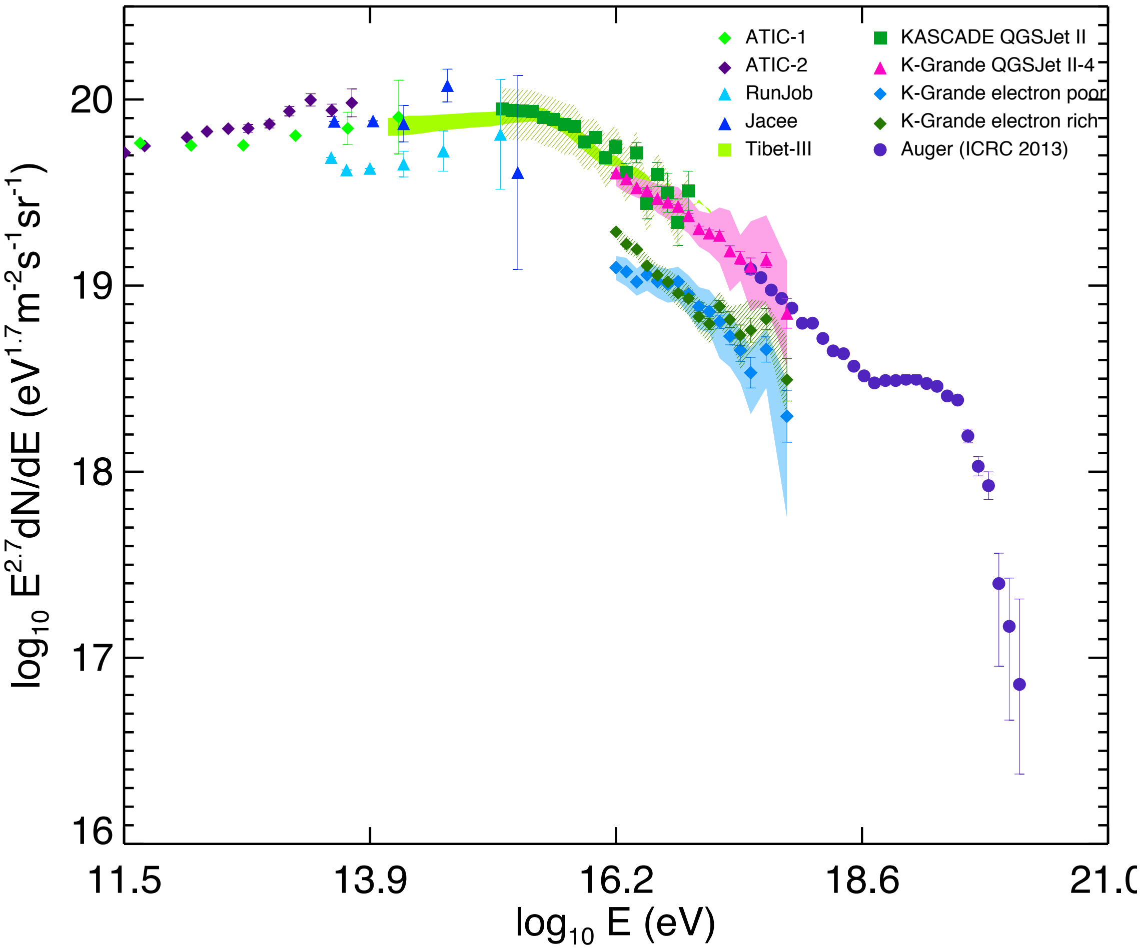

Consequences for UHECR phenomenology: extragalactic UHECRs

The heavy knee and the light ankle
$E \sim 10^{17}$ eV

KG showed evidence for an “ankle” in the light component

If the transition between GCR and eGCRs arises at the ankle (mixed composition), a likely explanation is: an extragalactic light component is starting to emerge on top of the light galactic component

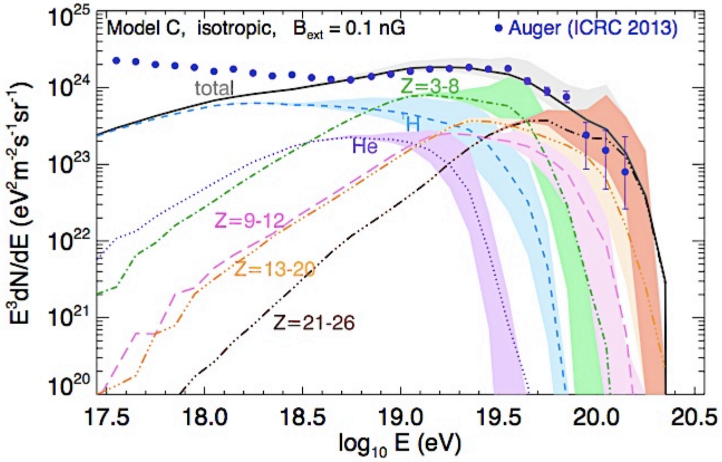

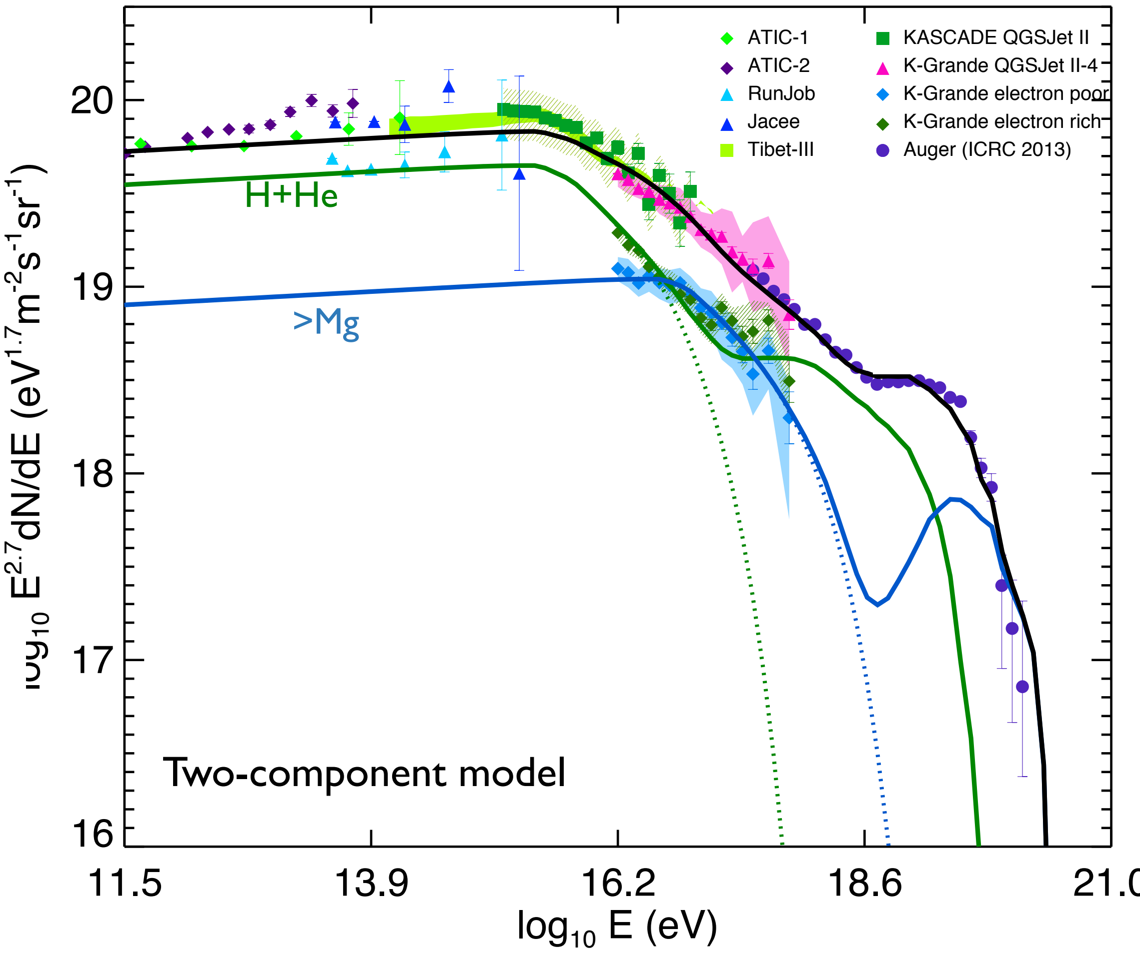

please check
Globus, Allard & Parizot 2015
Phys. Rev. D 92, 021302 (Rapid Com)

Consequences for UHECR phenomenology: Galactic UHECRs

Test particle simulations show that the escape rate from the Galaxy at near-ankle energies is nearly proportional to E/Q (Figure 5 of Kumar and Eichler, 2014)

If UHECRs are due to Galactic GRBs then a softer proton component and the rigidity dependent escape at the sources can explain an ankle-like feature

Another Galactic component needed below ~10^{17} eV

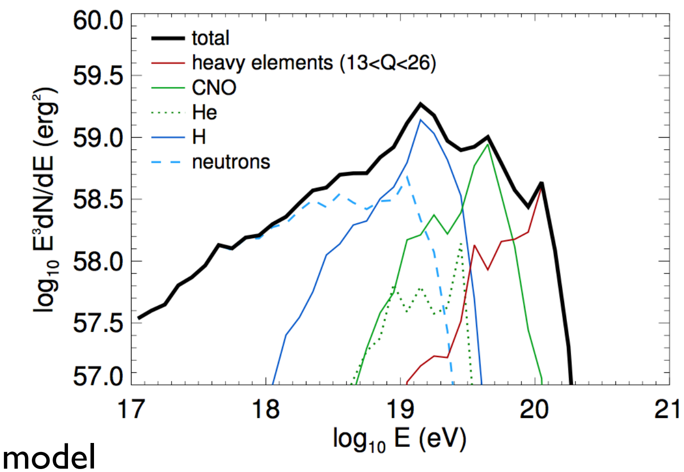

Galactic model

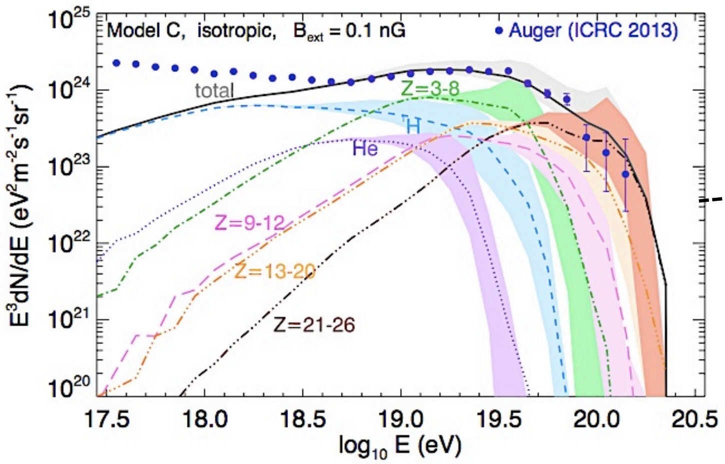

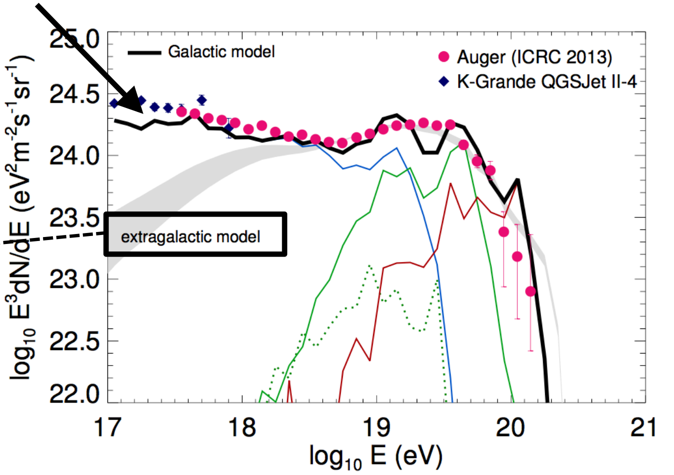

please check
Eichler, Globus, Kumar, Gavish, 2016,
ApJ Letters, 821, 24

Modeling the Cosmic Rays primary observables

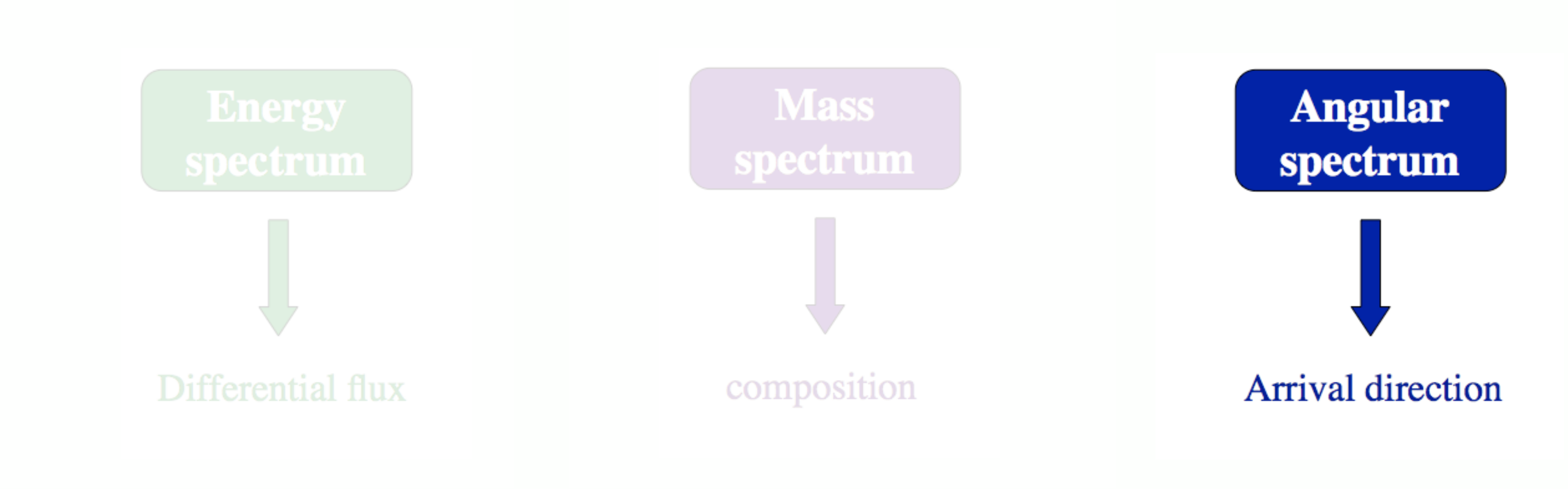

Energy spectrum

Differential flux

Mass spectrum

composition

Angular spectrum

Arrival direction

The GMF of the Milky Way

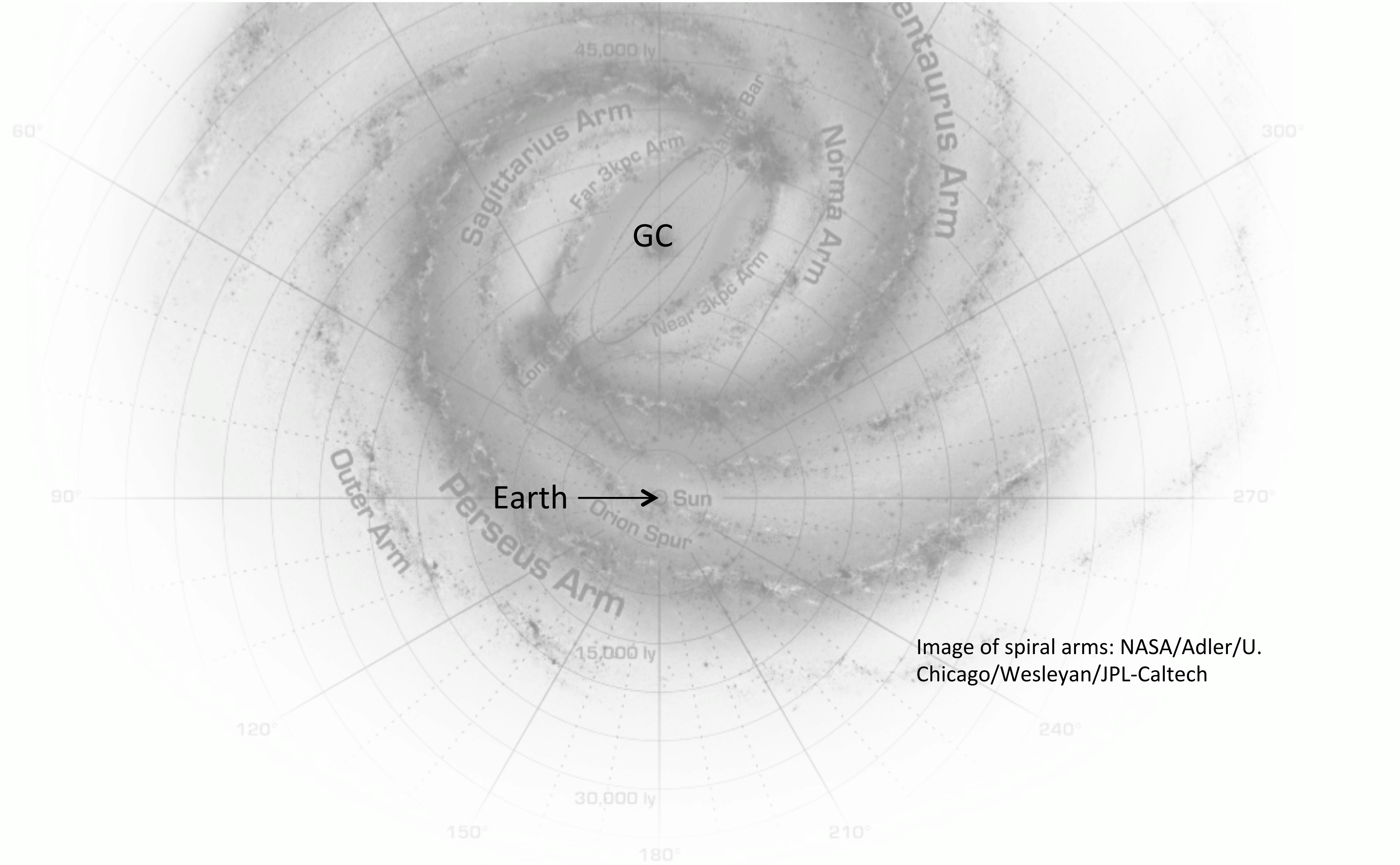

Image of spiral arms: NASA/Adler/U. Chicago/Wesleyan/JPL-Caltech

The GMF of the Milky Way

Jansson & Farrar 2012

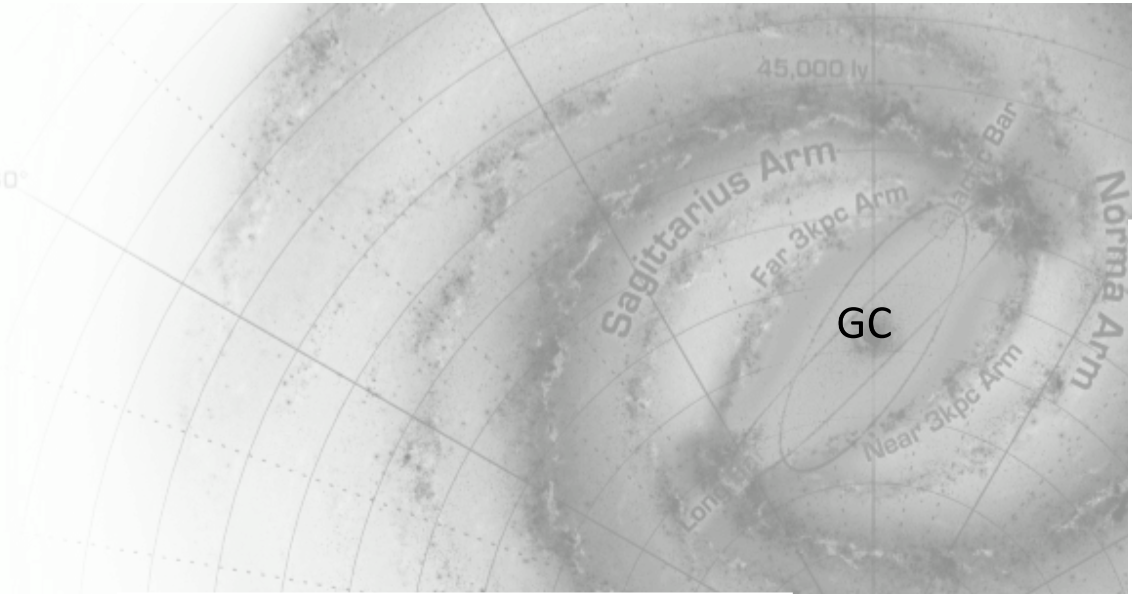

GMF: regular component

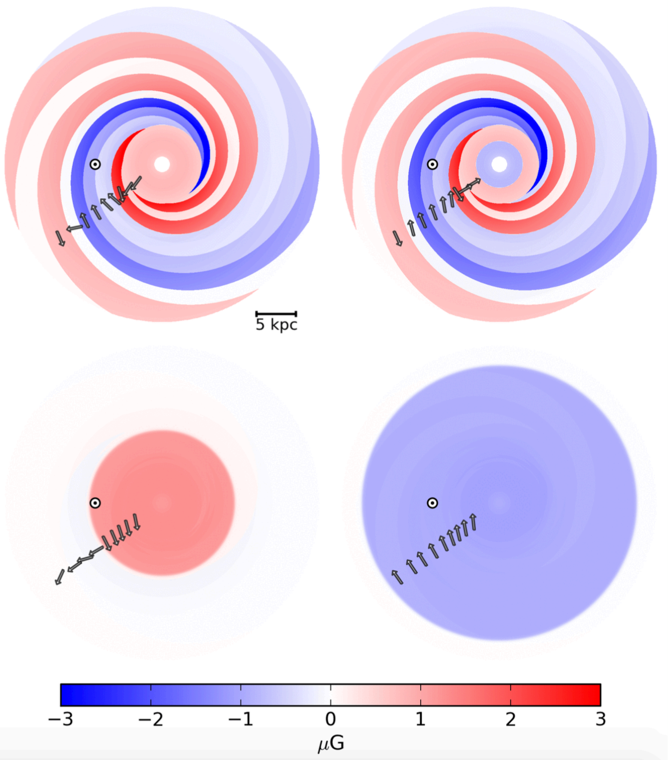

GMF: regular component

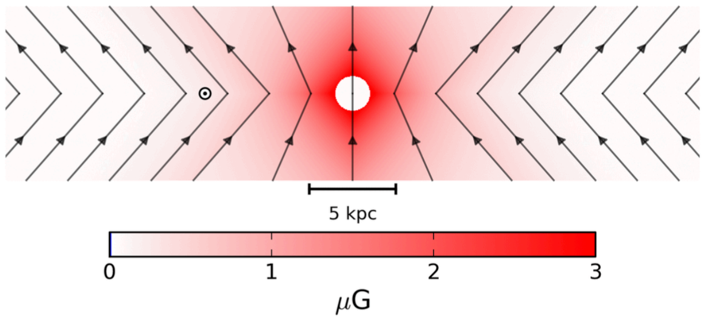

The GMF of the Milky Way

Jansson & Farrar 2012

regular, large scale coherent field

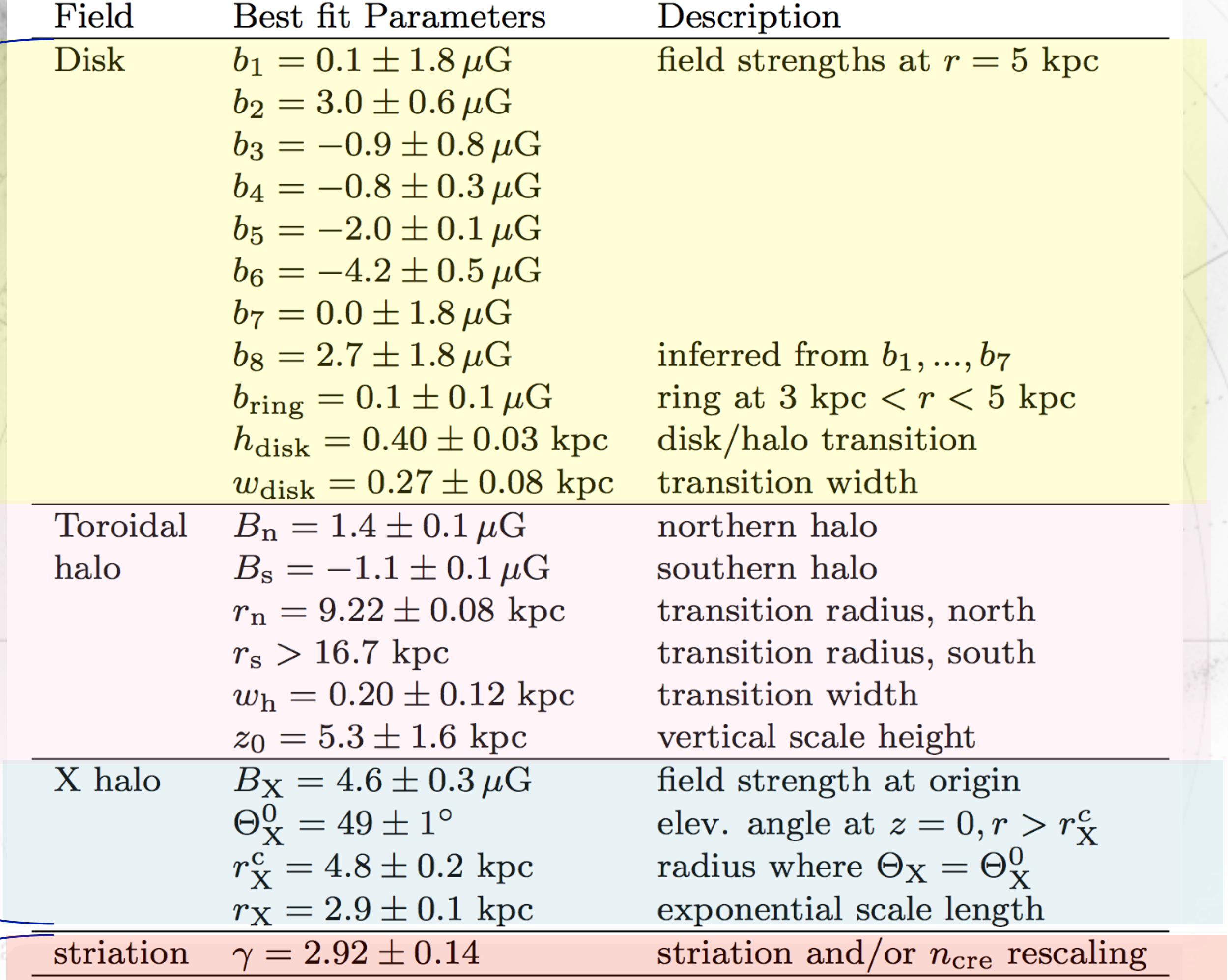

Field	Best fit Parameters	Description
Disk	$b_1 = 0.1 \pm 1.8\,\mu\mathrm{G}$	field strengths at $r = 5$ kpc
	$b_2 = 3.0 \pm 0.6\,\mu\mathrm{G}$	
	$b_3 = -0.9 \pm 0.8\,\mu\mathrm{G}$	
	$b_4 = -0.8 \pm 0.3\,\mu\mathrm{G}$	
	$b_5 = -2.0 \pm 0.1\,\mu\mathrm{G}$	
	$b_6 = -4.2 \pm 0.5\,\mu\mathrm{G}$	
	$b_7 = 0.0 \pm 1.8\,\mu\mathrm{G}$	
	$b_8 = 2.7 \pm 1.8\,\mu\mathrm{G}$	inferred from $b_1, ..., b_7$
	$b_{\mathrm{ring}} = 0.1 \pm 0.1\,\mu\mathrm{G}$	ring at $3\ \mathrm{kpc} < r < 5$ kpc
	$h_{\mathrm{disk}} = 0.40 \pm 0.03$ kpc	disk/halo transition
	$w_{\mathrm{disk}} = 0.27 \pm 0.08$ kpc	transition width
Toroidal halo	$B_{\mathrm{n}} = 1.4 \pm 0.1\,\mu\mathrm{G}$	northern halo
	$B_{\mathrm{s}} = -1.1 \pm 0.1\,\mu\mathrm{G}$	southern halo
	$r_{\mathrm{n}} = 9.22 \pm 0.08$ kpc	transition radius, north
	$r_{\mathrm{s}} > 16.7$ kpc	transition radius, south
	$w_{\mathrm{h}} = 0.20 \pm 0.12$ kpc	transition width
	$z_0 = 5.3 \pm 1.6$ kpc	vertical scale height
X halo	$B_{\mathrm{X}} = 4.6 \pm 0.3\,\mu\mathrm{G}$	field strength at origin
	$\Theta^0_{\mathrm{X}} = 49 \pm 1°$	elev. angle at $z = 0, r > r^c_{\mathrm{X}}$
	$r^c_{\mathrm{X}} = 4.8 \pm 0.2$ kpc	radius where $\Theta_{\mathrm{X}} = \Theta^0_{\mathrm{X}}$
	$r_{\mathrm{X}} = 2.9 \pm 0.1$ kpc	exponential scale length
striation	$\gamma = 2.92 \pm 0.14$	striation and/or n_{cre} rescaling

turbulent field

+ purely turbulent magnetic field (Kolmogorov) with coherence length of 50-200 pc (Beck+2012) and r.m.s. value of 3 times the magnitude of the regular component

Including the GMF : Jansson & Farrar 2012

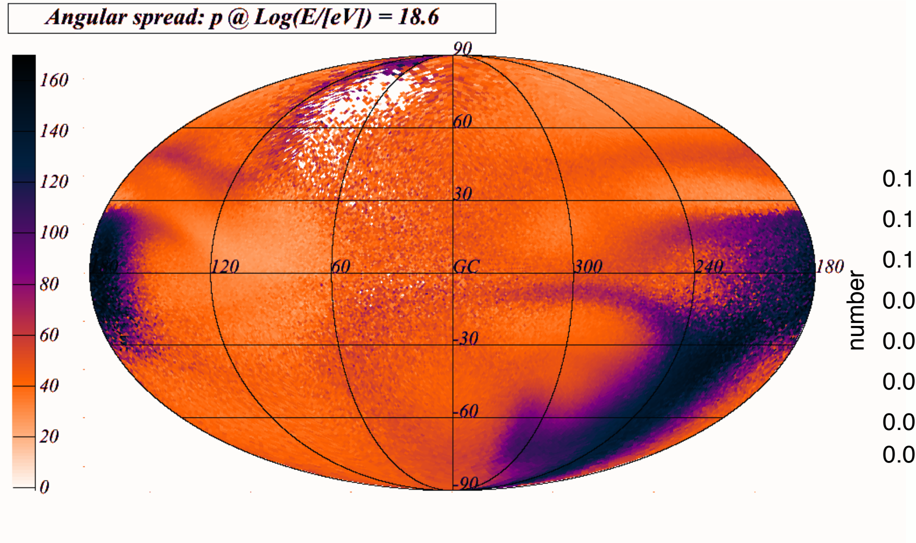

Angular spread (spot size)

from back propagation (Rouillé d'Orfeuil et al. 2014)

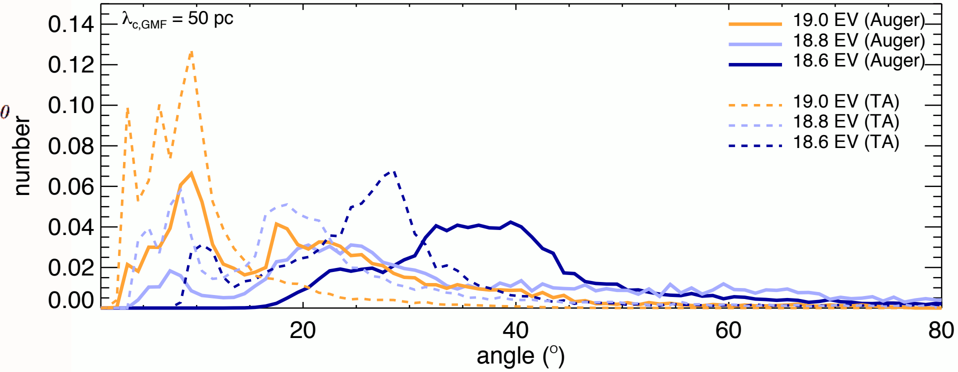

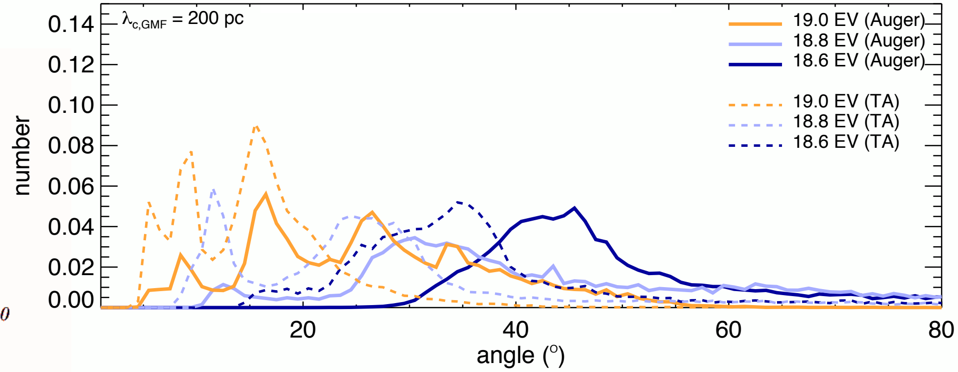

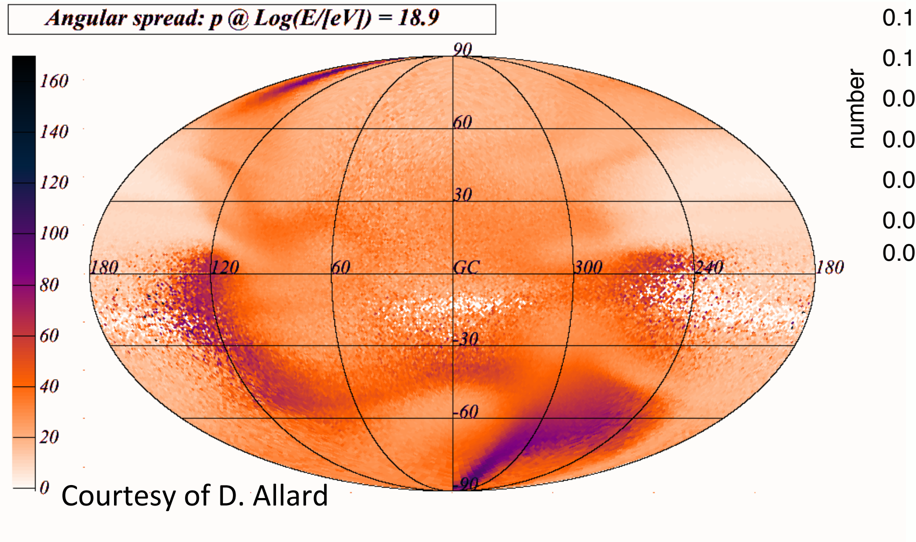

Courtesy of D. Allard

Including the GMF : Jansson & Farrar 2012

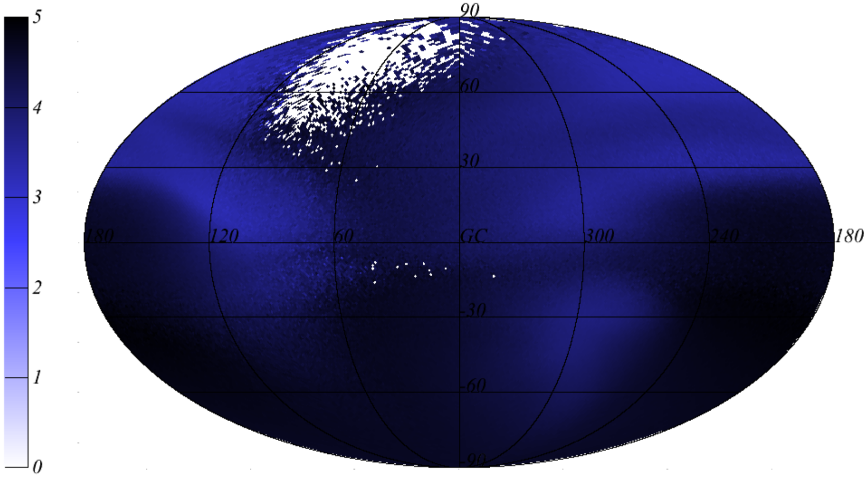

Mean time delay (log(year)): p @ Log(E/[eV]) = 186

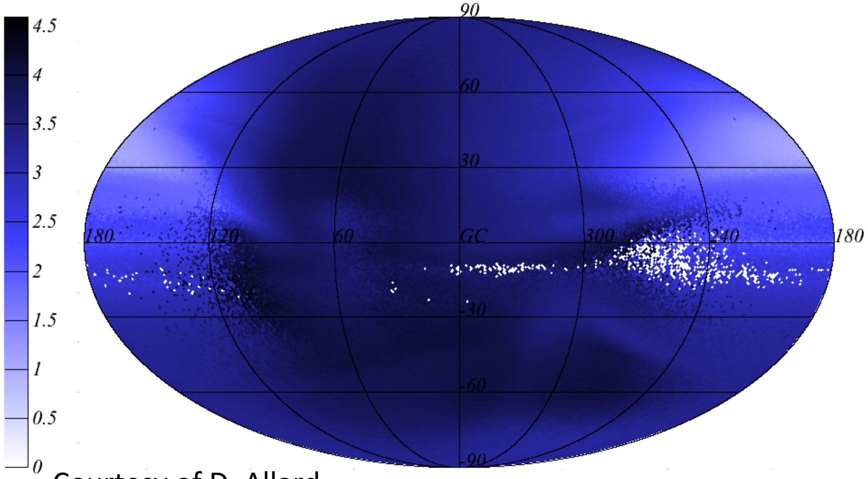

Mean time delay (log(year)): p @ Log(E/[eV]) = 190

Courtesy of D. Allard

time delay

from back propagation (Rouillé d'Orfeuil et al. 2014)

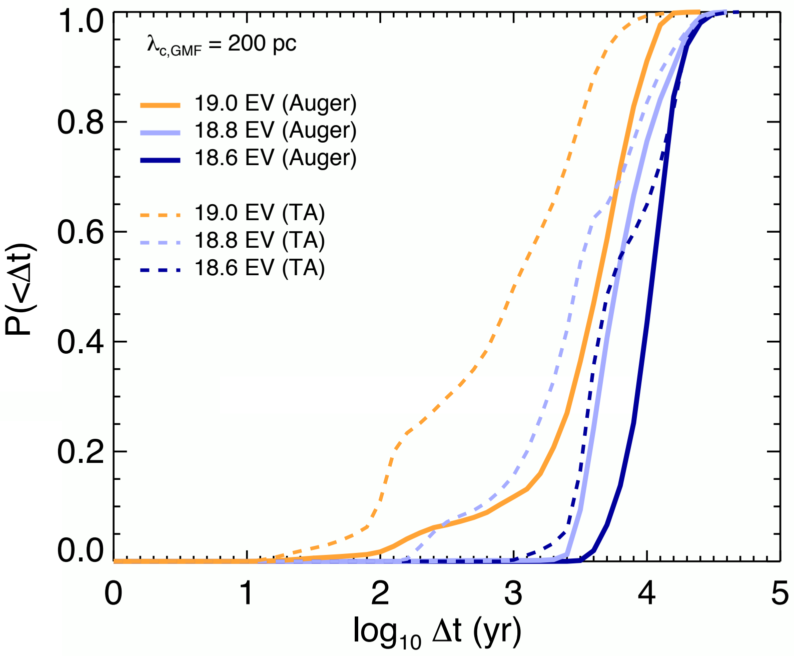

UHECR trajectories in the GMF

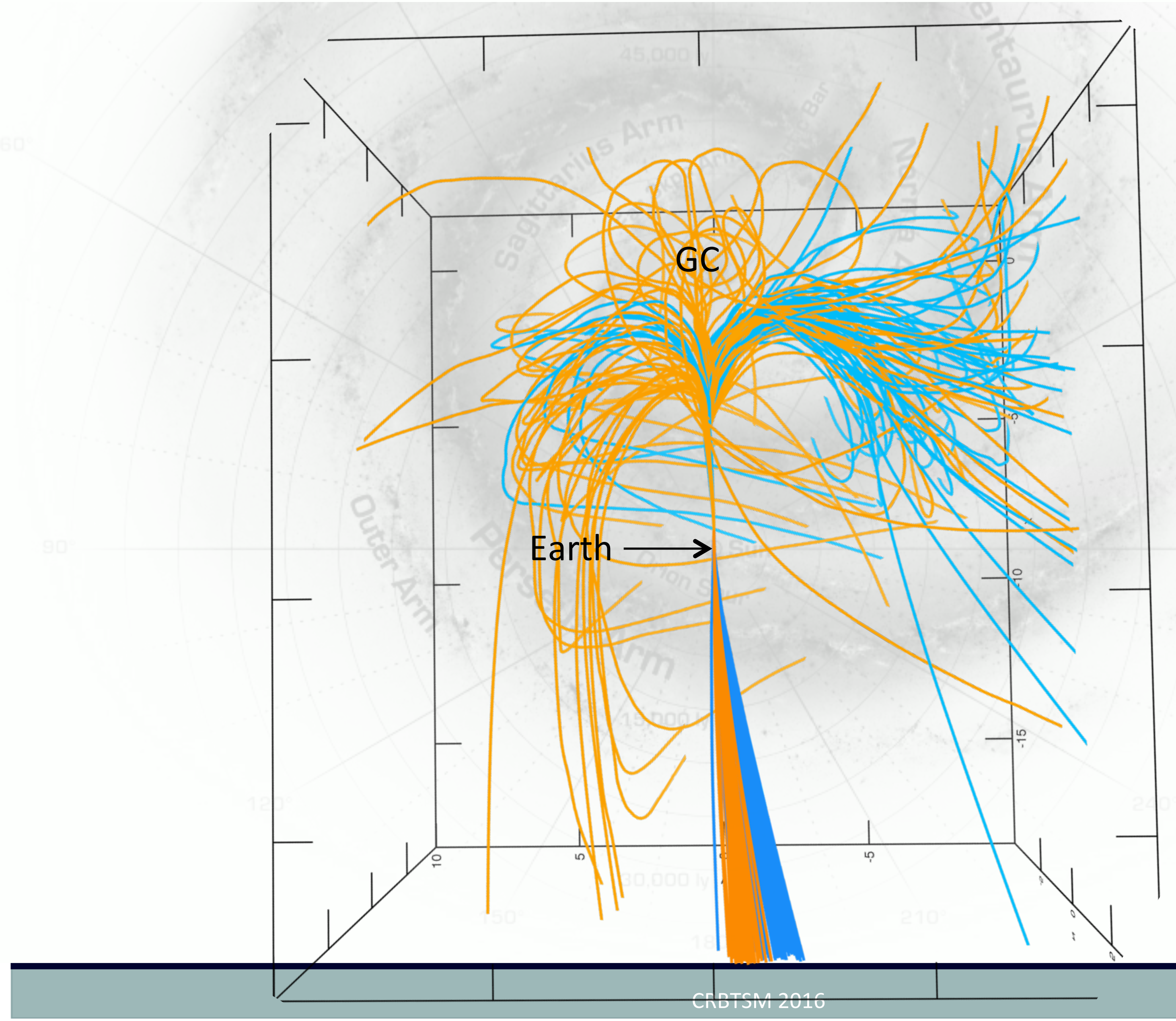

ρ = 3 EV

2 configurations of the magnetic turbulence

l= 0° (Galactic center)

l= 180° (anticenter)

b= 90°

UHECR trajectories in the GMF

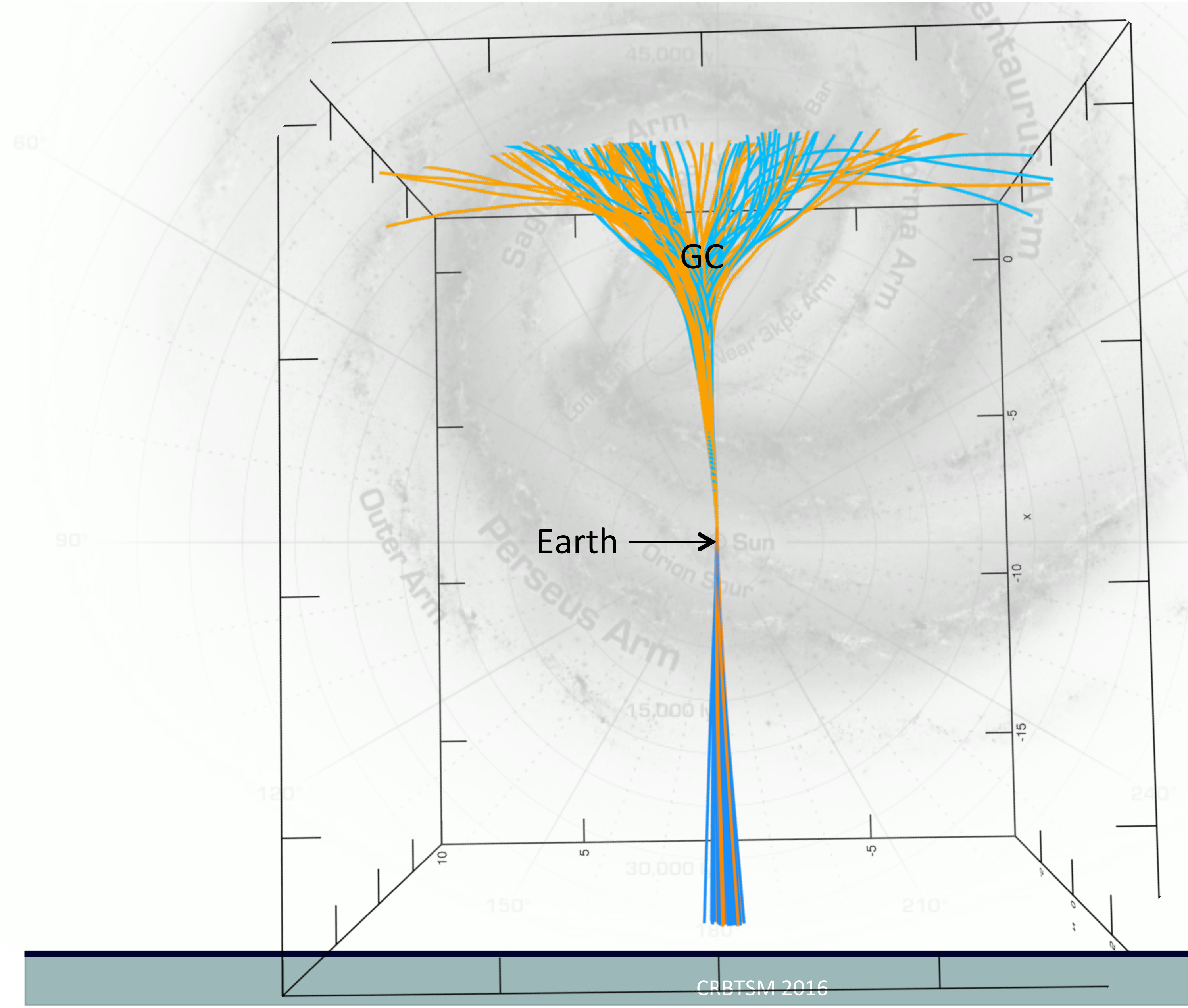

ρ = 10 EV

2 configurations of the magnetic turbulence

l= 0° (Galactic center)

l= 180° (anticenter)

b= 90°

Angular decorrelation due to Earth's motion (5 years)

Globus & Eichler, in preparation

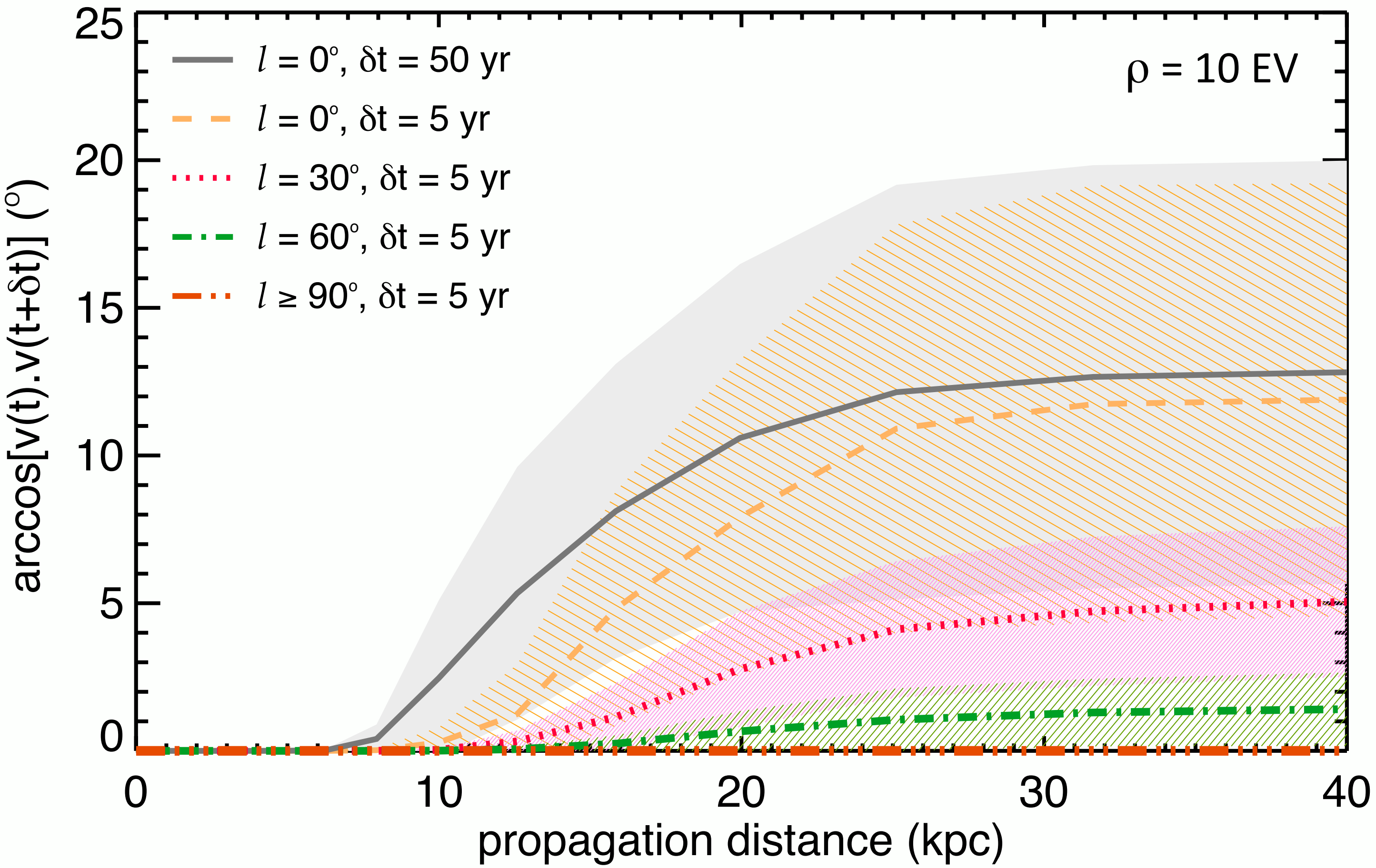

Skymap production (extragalactic GRBs)

Globus, Allard, Parizot, Lachaud & Piran, in final shaping

1200 realizations of the history of GRB explosions in the Universe

Propagation in extragalactic turbulent magnetic field, including energy losses on extragalactic photon backgrounds and in Galactic magnetic field (back propagation)

Probability distribution of energies P(E), redshifts P(z; E), sources P(S; z, E), masses P(A; z, E, S), deflection angles P(Δθ; z, E, S, A)

For each realization, we calculate the total spectrum, and according to this spectrum and the pre-calculated probability tables, we draw first the energy, the redshift, the source, the mass and charge of the particle, and the deflection Δθ which give the position of the source. Then we take into account the GMF (magnifications + deflections see Rouillé d'Orfeuil et al., 2014)

We then produce data sets (10 per realization) with Auger and TA statistics, exposure and resolution, above 5 EeV

Skymaps are built out of the 83 and 231 highest energy events for TA and Auger, respectively

Resulting UHECR propagated spectrum (extragalactic GRBs)

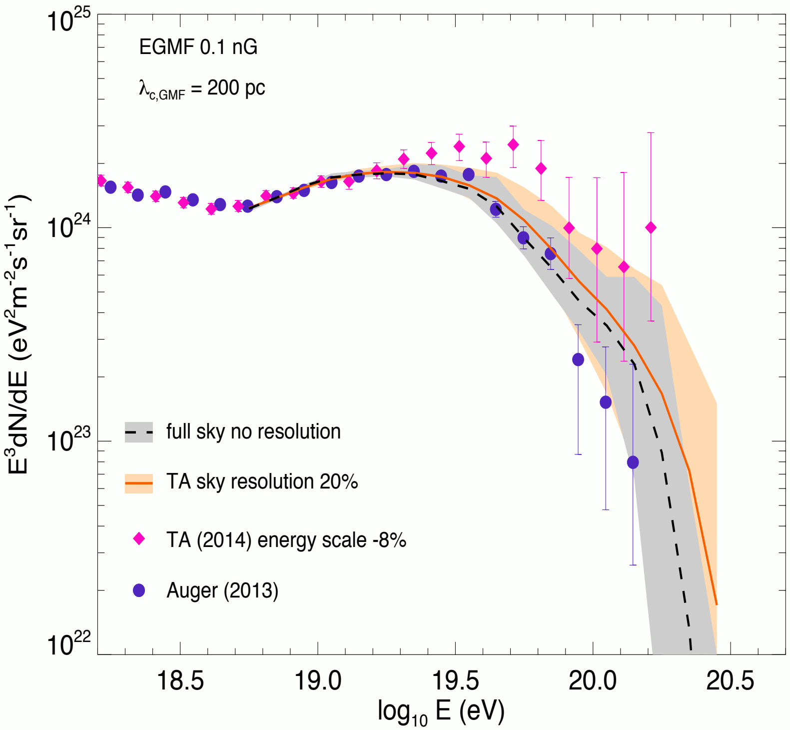

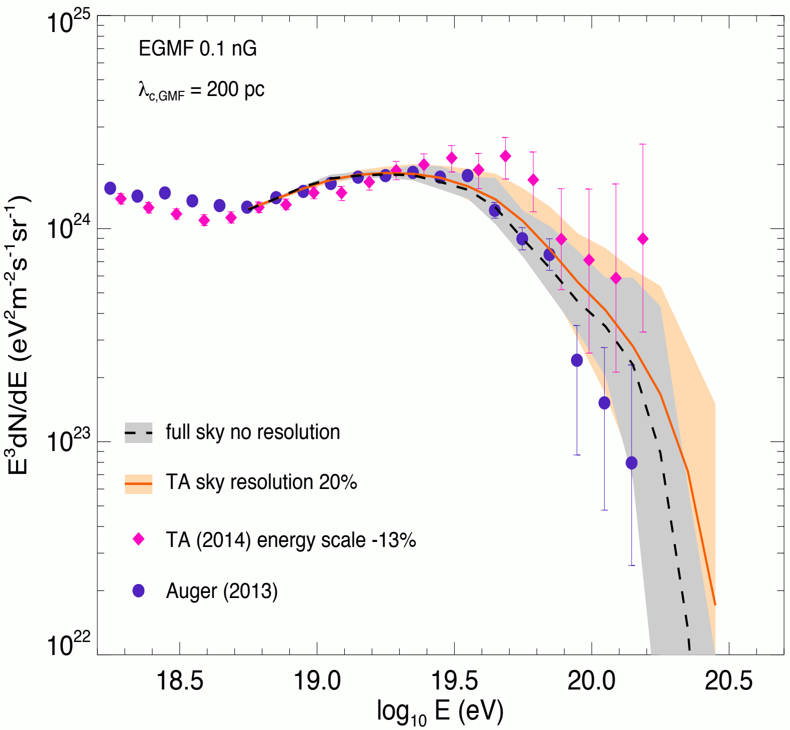

Our average energy spectrum is compatible with the Auger data.
Is it possible to account for both Auger and TA observations ?

E_{83} and E_{231} probability distributions

Globus, Allard, Parizot, Lachaud & Piran, in final shaping

TA: 83 above 57 EeV
Auger: 231 above 52 EeV

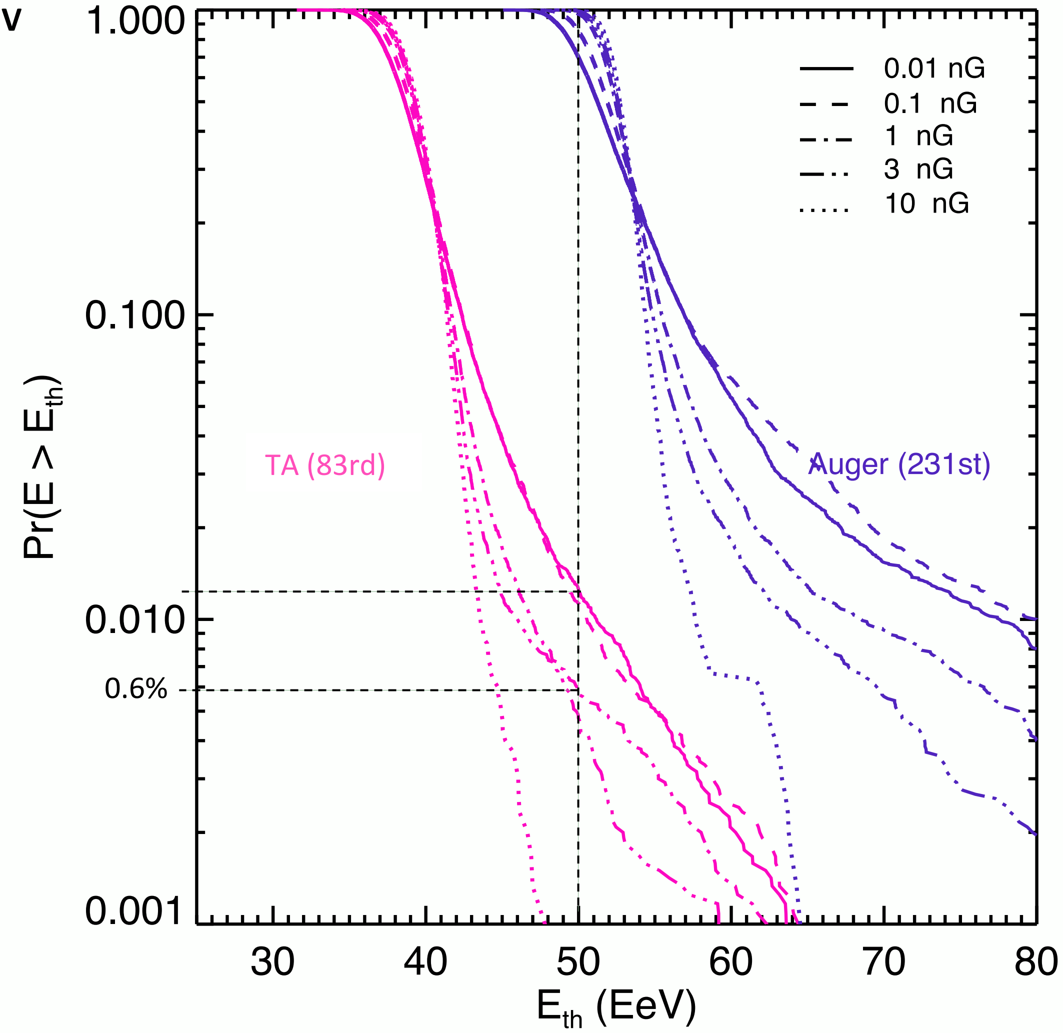

1200 realisations of the history of GRB explosions in the Universe

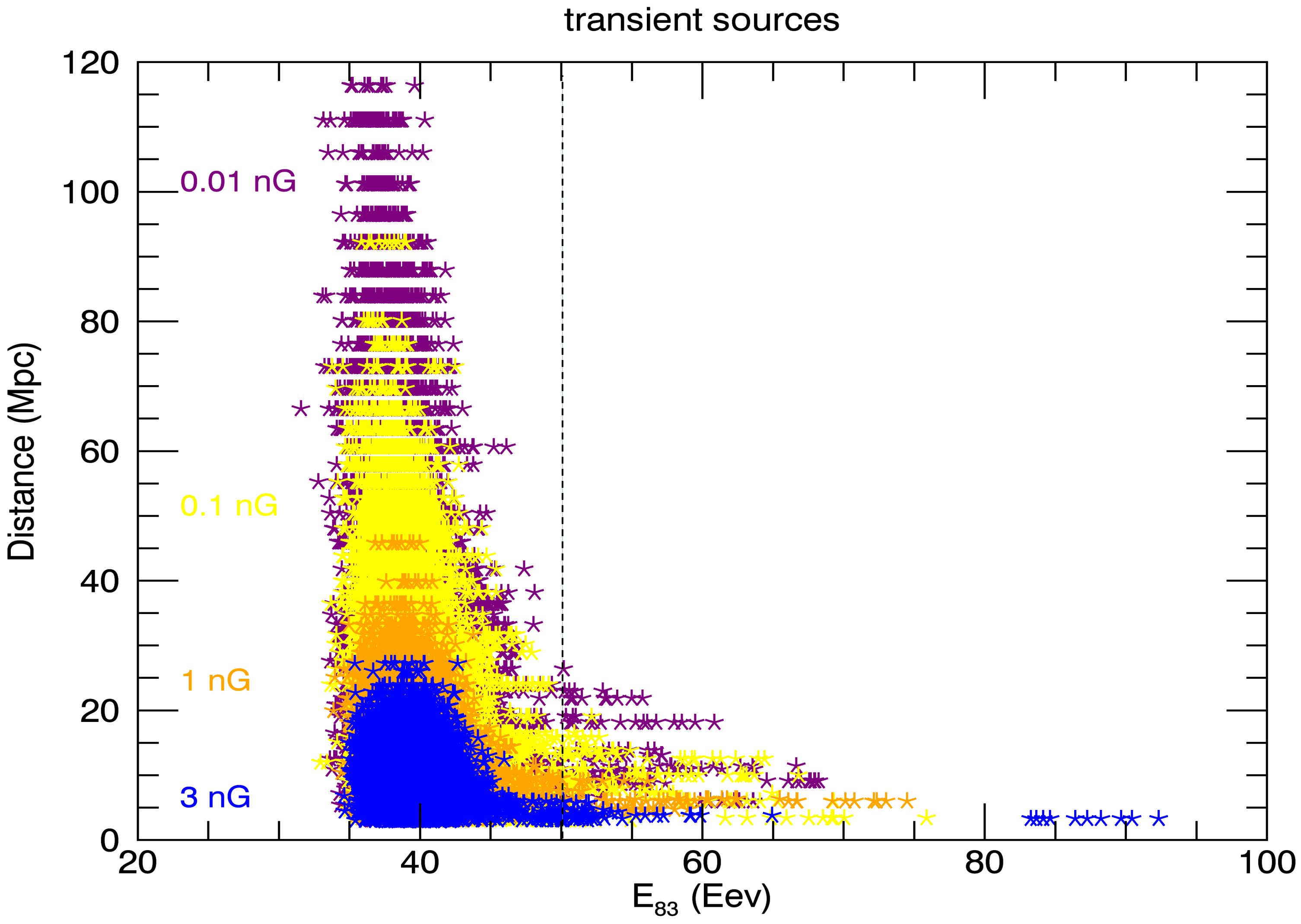
transient sources
Distance (Mpc)
E_{83} (Eev)
0.01 nG
0.1 nG
1 nG
3 nG
0
20
40
60
80
100
120
20
40
60
80
100

Probability to fit the 2pt correlation function

Globus, Allard, Parizot, Lachaud & Piran, in final shaping

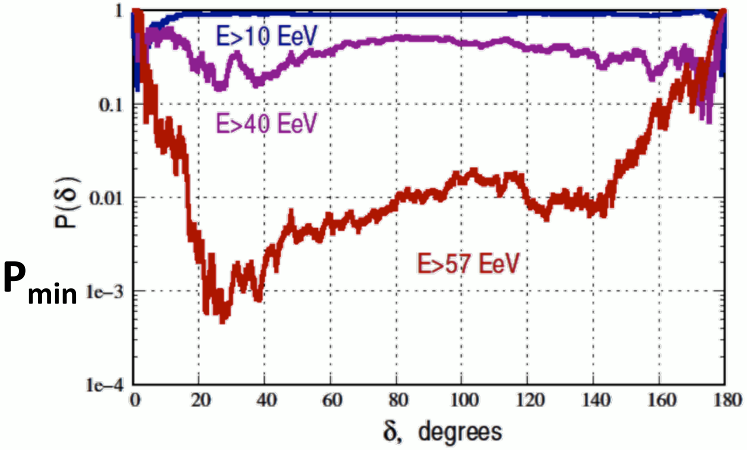

For each angular bin:

1. Count number of pairs of events at in the bin at separation δ
2. Chance Probability is given by the fraction of isotropic MC sets (with equal statistics) with as many or more than the number of pairs seen in data

Compatible with isotropy at E > 10 EeV and E > 40 EeV,
Tension with isotropy at E>57 EeV

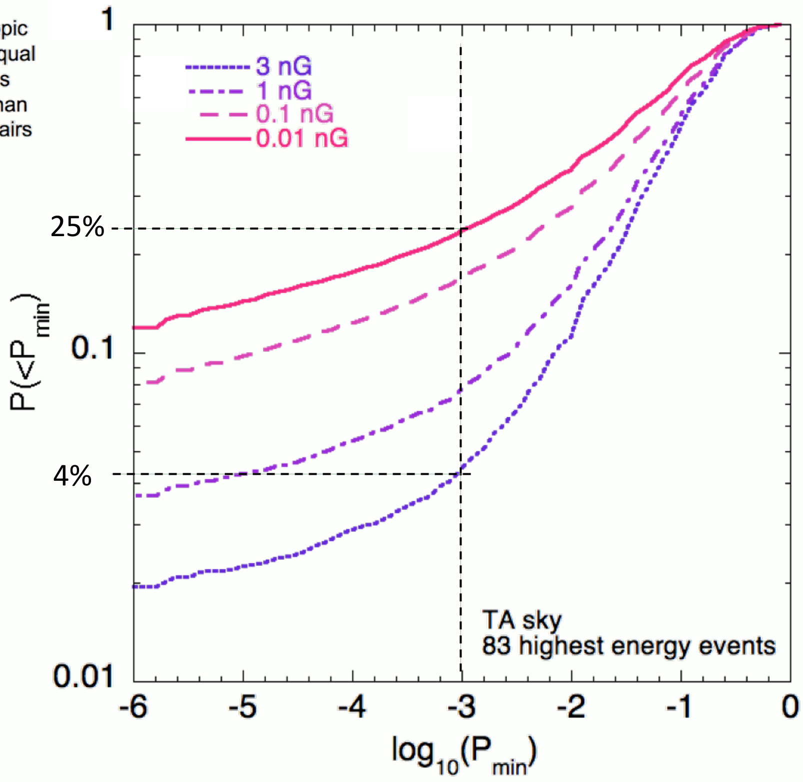

1200 realisations of the history of GRB explosions in the Universe

Realization that account for the excess and the anisotropy

B_{EGMF} = 3 nG

76 evts > 50 EeV @20 degrees 4.8σ (20 evts)
2pt 4.e-5 (23 degrees)

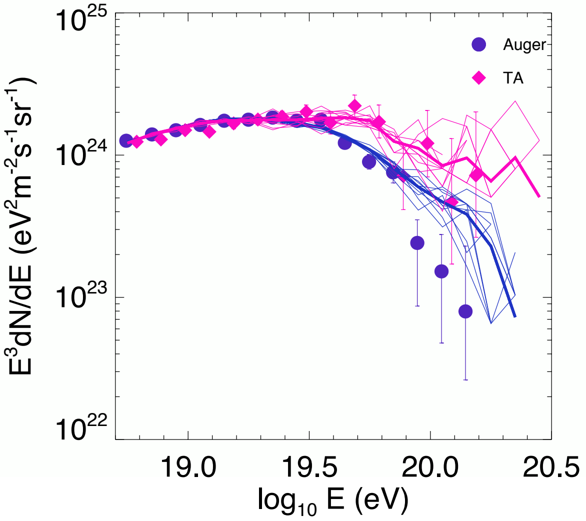

TA

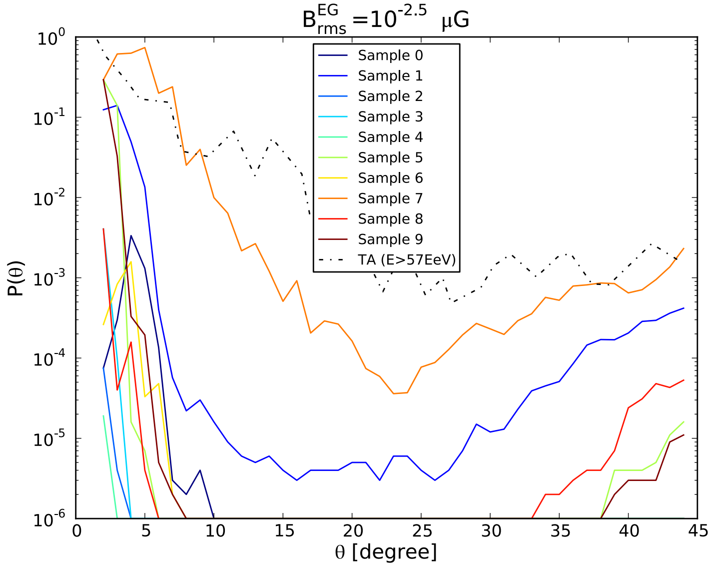

Auger

TA

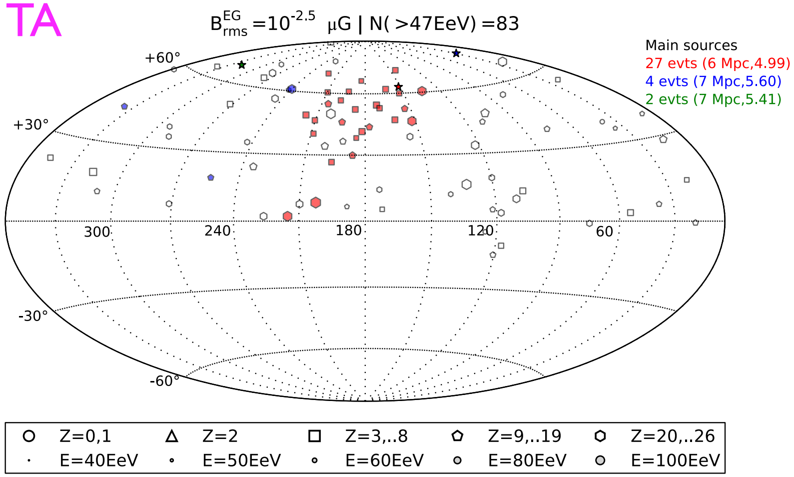

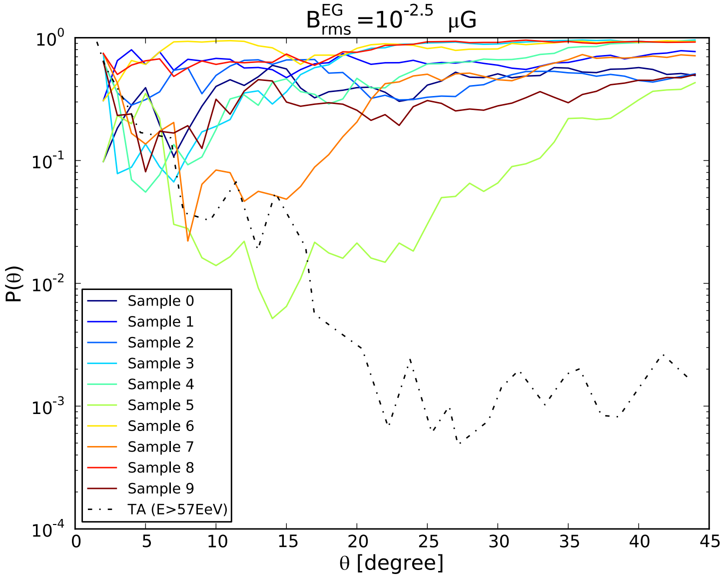

Realization that account for the excess and the anisotropy

B_{EGMF} = 3 nG

76 evts > 50 EeV @20 degrees 4.8σ (20 evts)
2pt 4.e-5 (23 degrees)

TA

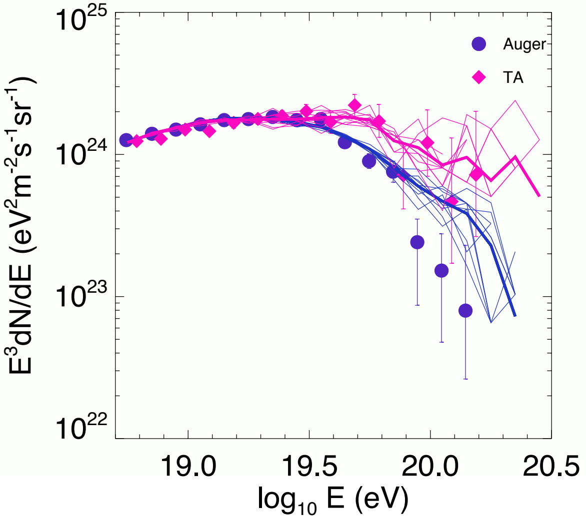

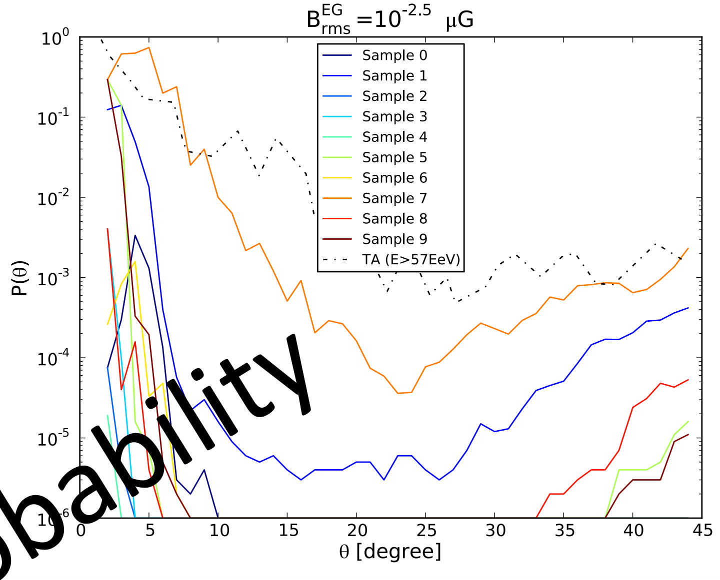

very low probability

Auger

TA

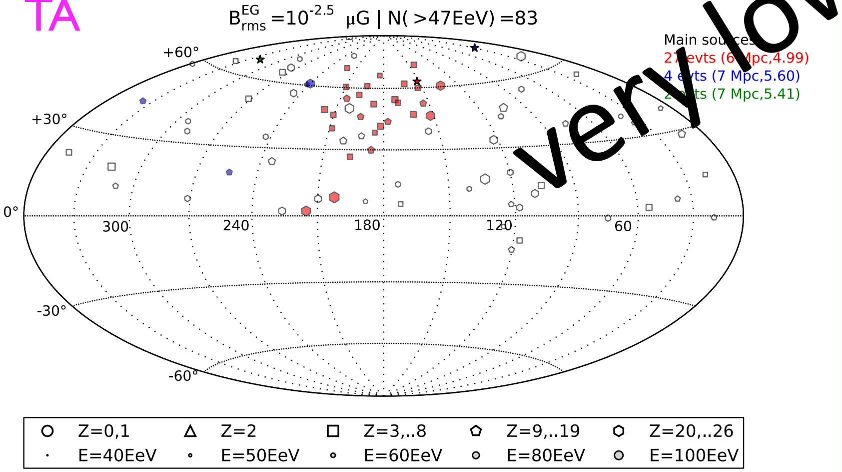

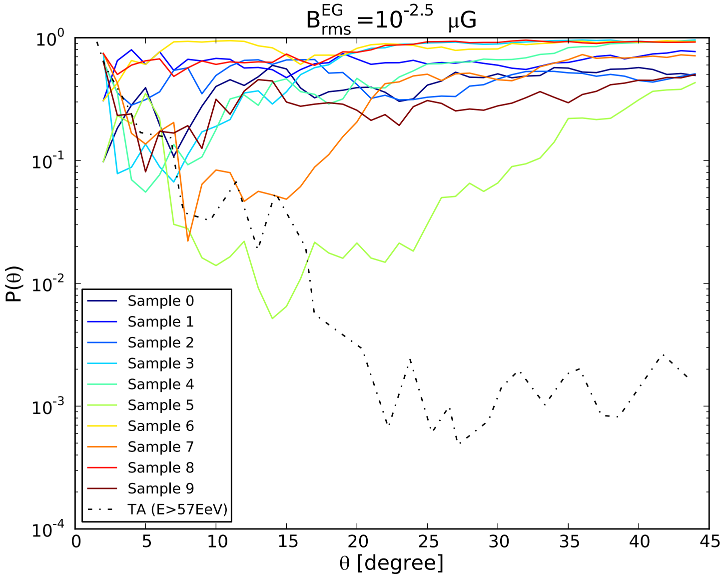

Preliminary conclusions

The anisotropy level seen by TA (hot spot of angular scale 20 degrees) is not the one that is expected given the difference between the Auger and TA spectra

In the case of bursting sources**, the probability to account for both the excess and the anisotropy (Auger + TA) is very low (below 0.1%)**

We stress that it is unlikely to recover the excess in the spectrum for too strong extragalactic magnetic fields (>10 nG), because too many sources would contribute to the flux at a given time.

If $B_{EGMF} < 0.3$ nG), the effect of the GMF becomes dominant in terms of angular spread (Jansson and Farrar model)

In the case of steady sources, **the probability to account for the TA excess in the spectrum is ~5% for a source density of 10^{-5} Mpc^{-3}. In that case the typical source distance is less than ~30 Mpc.**

It should be also kept in mind that we used an homogeneous extragalactic magnetic field and that large magnetic structures could also play an important role on the observed anisotropy level